Canadian Science Publishing | Canadian Journal of Civil Engineering

# Discharge estimation in non-prismatic compound channel using adaptive neuro-fuzzy inference system

| | |
|---|---|
| Journal: | *Canadian Journal of Civil Engineering* |
| Manuscript ID | cjce-2018-0038.R1 |
| Manuscript Type: | Article |
| Date Submitted by the Author: | 31-Jul-2019 |
| Complete List of Authors: | Das, Bhabani Shankar; National Institute of Technology Rourkela, Civil Engineering<br>Devi, Kamalini; Vidya Jyothi Institute of Technology, Civil Engineering<br>Khuntia, Jnana Ranjan; National Institute of Technology Rourkela, Civil Engineering<br>Khatua, Kishanjit Kumar; National Institute of Technology Rourkela, Civil Engineering |
| Keyword: | non-prismatic compound channel, ANFIS, Gamma test, M-test, ANN |
| Is the invited manuscript for consideration in a Special Issue? : | Not applicable (regular submission) |

# Discharge estimation in converging and diverging compound open channels by using adaptive neuro-fuzzy inference system

B. S. Das[1], K. Devi[2], J. R. Khuntia[3], K. K. Khatua[4]

[1]*Assistant Professor, Civil Engineering Department, TIET Patiala, India*

[2]*Associate Professor, Civil Engineering Department, VJIT Hyderabad, India*

[3]*Ph.D. Scholar, Civil Engineering Department, NIT Rourkela, India*

[4]*Associate Professor, Civil Engineering Department, NIT Rourkela, India*

*Corresponding author Email:* bsd.nitrkl@gmail.com

**ABSTRACT**

The computation of total flow in a flooded river is very crucial work in designing economical flood defense schemes and drainage systems. Further, under non-uniform flow conditions like in converging and diverging compound channel, the traditional methods provide poor results with high errors. The analytical methods require the system of non-linear equations to be solved which are very complex. So, mathematical models that prompt in taking care of complex system of problem are solved here through an artificial neural network (ANN) and adaptive neuro-fuzzy inference system (ANFIS). By utilizing ANN and ANFIS, an attempt is taken to predict the discharge in converging and diverging compound channel. In the analysis, the most influencing dimensionless parameters such as friction factor ratio, area ratio, hydraulic radius ratio, bed slope, width ratio, relative flow depth, angle of converging or diverging, relative longitudinal distance, flow aspect ratio are taken into consideration for computation of discharge. Gamma test and M test have been performed to achieve the best combinations of input parameters and training length respectively. The significant input parameters that influence the discharge are found to be friction factor ratio, hydraulic radius ratio, relative flow depth, and bed slope. A suitable performance is achieved by the ANFIS model as compared to ANN model with a high coefficient of determination of 0.86 and low root mean square error of 0.005 in predicting the discharge of non-prismatic compound channels taken under consideration.

*Keywords: Non-prismatic compound channels; Gamma Test, M test, relative flow depth; width ratio, relative flow depth; ANN, ANFIS*

## 1 Introduction

The sustainability of human civilization depends on rivers due to the availability of water for their day-to-day activity. But the same river devastates everything and causes the loss of life during the flood by inundating the surrounding floodplains. Because of the settlements on the adjoining area, the floodplain widths are found to be increased at some places and reduced at some other places. These configurations provide the floodplain either a converging or a diverging geometry is known as non-prismatic floodplains. Hence the flow will be non-uniform due to the non-uniform cross sections. So, the estimation of the proper discharge in non-prismatic sections is significant for analyzing the flow as they imitate the natural rivers. There are many investigators devoted their research on the prismatic compound channel to analyse the flow (Sellin 1964; Wormleaton et al. 1982; Knight and Demetriou 1983; Knight et al. 1989; Devi et al. 2016). But very few investigations have been carried out on the non-prismatic compound channel. The experiment in a skewed compound channel has been first performed by James and Brown (1977) considering different skew angles. Later the effect and the behaviour of energy slope in skewed compound channels were studied by Chlebek (2009). Shiono et al. (1999) preformed experiments to examine the flow behaviors in a meandering compound channel. But very few numbers of researches have been done for converging and diverging compound channel cases. Converging compound channels with three different angles have first been studied by Bousmar et al. (2002). An asymmetric compound channel with abrupt floodplain contraction with a converging angle 22° was studied by Proust (2005). A comparison study of flow behavior between converging and diverging compound channels were done by Bousmar et al. (2006) by conducting experiments in diverging compound channels. An analytical model for computing water surface profile was developed by Rezaei (2006) based on the experiment in converging compound channel (Fig. 1a). Utilizing the first law of thermodynamics, a one-dimensional energy loss model was developed by Proust (2010). Though this model predicts the energy loss in each subsection (i.e., left floodplain, main channel and right floodplain) however the method is complex and contains calibrating coefficients and also not shows good results for all the relative flow depths. However, due to its complexity and requirement of calibrating coefficients, the model results are found to be not satisfactory for different types of flow depths. As it depends upon calibrating coefficients improper approximation coefficients will lead to inaccurate results. So the requirement of a better model has been felt which can predict discharge well for these non-prismatic types compound open channels.



In the last two and a half decades, many artificial intelligence (AI) techniques have been used to compute the discharge capacity of the channel. MacLeod (1997); Liu and James (2000) used artificial neural networks (ANN) for flow discharge calculation of meandering compound channels. Zahiri and Dehghani (2009); Unal et al. (2010) used ANN for discharge prediction in a straight compound channel. Parsaei et al. (2017) used ANFIS to predict discharge in prismatic compound channels. Some of the pertinent works based on time series data as an input to ANN include forecast prediction using time series analysis by Hsu et al. (1995). ANN and ANFIS model used by Yarar et al. (2009) to predict water level changes in lake and Vafakhah (2012) used to forecast short term flow. Dorum et al. (2010) used ANFIS to model rainfall-runoff data.

Here, in this paper, an attempt has been made to use AI techniques in non-prismatic type compound open channel to solve the complex flow problems and compared with traditional discharge estimating approaches. Two AI techniques such as ANN and ANFIS have been used to develop models which can able to predict the discharge in converging and diverging type compound channels (Fig. 1b). Between these two models, the most reliable model is suggested at the end of this paper for this type of compound open channels.

Fig. 1. Schematic diagram of the non-prismatic compound channel, (a) converging compound channel ($\theta$=3.81°), (Rezaei 2006) and (b) diverging compound channel ($\theta$=3.81°), (Yonesi et al. 2013)



## 2 Methodology

In this section, firstly the four traditional approaches are presented which are generally used to calculate discharge at different sections. Secondly, Gamma test and M-test have been carried out to select the most influencing input parameters and training data length, respectively to develop ANN and ANFIS model.

### 2.1 Traditional Approaches

#### *2.1.1. Single channel method (SCM)*

In this method, the whole compound channel is taken as a single unit. The same formulae are executed for both the simple and compound river channel. The disadvantages of this method are erroneous computation of discharge in the compound river channel. This is due to the fact that when the water level rises and inundates the floodplain, wetted perimeter as compared to wetted area suddenly increases in a higher order which leads to under-estimation of the discharge. Thus the discharge computed by SCM is always less than the actual discharge values. Generally, the Manning's formula is used for determining the discharge and given by

$$Q = \frac{1}{n} A R^{2/3} \sqrt{S_0} \tag{1}$$

where $Q$ - total discharge, $n$ is the equivalent roughness coefficients, $R$ is the hydraulic radius (= $A/P$ in which $A$ is cross-sectional area and $P$ is wetted -perimeter), $S_0$ is bed slope.



### *2.1.2 Divided Channel method (DCM)*

First, Lotter (1933) developed a method for prediction of discharge in compound channels by dividing the whole compound section into different parts like a left floodplain, main channel and right floodplain. By introducing division lines such as vertical, horizontal and diagonal lines he separated by assuming homogenous velocities in each subsection. Then individual discharges are found out by applying Manning's equation (Equation 1) in every sub section and total discharge is assessed by adding all individual discharge together.

Figure 2. Kinds of isolating limit between the main channel and floodplains. (Parsaei et al., 2017)

$$Q = \sum_{i=1}^{N} \frac{A_i R_i^{2/3}}{n_i} \sqrt{S_0} \tag{2}$$

where the subscript $i$ stands for subsection, $A_i$- area of each subsection, $Ri$- Hydraulic radius of each subsection. This method is familiar with many hydraulic engineers and widely adopted as a divided channel method. The divisional lines used are vertical, horizontal and diagonal plain which are drawn from the intersection between main chnnael and fllodplain as shown in Fig. 2. (Al-Khatib et al. 2012; Devi et al. 2016; Parsaie et al. 2017). It should be noted that these three types of interfaces either may be included or excluded into the wetted perimeter of the main river channel but never be considered with floodplain cases. Then the summed of the individual flows of each sub-section of a particular division line provide the total discharge for that divisional line method thus there are whole total six distinctive divided channel methods which are either included or excluded such as $DCM_{v\text{-}e}$, $DCM_{v\text{-}i}$, $DCM_{h\text{-}e}$, $DCM_{h\text{-}i}$, $DCM_{d\text{-}e}$, $DCM_{d\text{-}i}$. In this technique subscripts h, v, d refer to the partitioned line horizontal, vertical and diagonal respectively. Likewise, i and e refer to the line as included and excluded from the wetted border of the main channel. Many commercial softwares like HEC-RAS, Mike 11 and ISIS are based on these DCM (Atabay and Knight 2006). Figure 3 shows the detailed methodology used in this study to develop a discharge predictive model.

Fig. 3. Flow chart of methodology used to develop a discharge predictive model

### *2.1.3 Interacting Divided Channel Method (IDCM)*

This method introduces a shearing at the vertical interface of the main channel and floodplain while computing the independent flow carried by subsections. It should be noted that it has been proposed to improve the divided channel method (Huthoff et al. 2008). The interface stress $\tau_{int}$ related to the momentum transfer is evaluated as

$$\tau_{\mathrm{int}} = \frac{1}{2}\gamma\rho\left(U_{mc}^{2} - U_{fp}^{2}\right) \quad (3)$$

where $\gamma = 0.02$ is a dimensionless exchange parameter, and $\rho = 1000$ kg/m$^3$ is the specific mass of water. The interface stress acts over a stature $H - h$. An advantage of IDCM is that it provides a direct analytical expression to determine the individual flow in subsections.

### *2.1.4 Exchange Discharge Model (EDM)*

Bousmar and Zech (1999) proposed the exchange discharge model where an extra loss in the head is taken into account that is added to the friction loss as determined from the divided channel method. This additional loss is corresponding to the exchange of energy at the junction region due to momentum transfer. Its magnitude is equal to velocity gradient times the discharge exchanges through the interface. They identified two distinct exchange discharge such as (1) a turbulent exchange discharge $q^t$, corresponding to the mass of water oscillating between subsections as a result of large-scale turbulence structures development; and (2) a geometrical transfer discharge $q^g$ found in non-prismatic or non-uniform flow, where discharge is forced through the interface as a result of cross-sectional area changes. The exchange discharges are estimated as follows:

$$q^{t} = \psi^{t}\left|\Delta U\right|\left(H - h\right) \text{ and } q^{g} = \psi^{g}\frac{dQ}{dx} \quad (4)$$

where $\psi^t = 0.16$ and $\psi^g = 0.5$ are fitting coefficients, fixed according to Bousmar&Zech (1999), and $h$= bank-full depth. Figure 4 shows the comparison between calculated discharges by analytical approaches and measured discharges.

Fig. 4. Comparison between the results of analytical approaches with the measured discharge

## 2.2 Gamma Test (GT)

Gamma test firstly reported by Agalbjörn et al. (1997) and later improved and examined in detail by numerous analysts (Durrant, 2001; Tsui et al., 2002). GT measures the base mean square error (MSE) that contribute to input data selections. The selected input data can be utilized as a part of an arrangement of a non-linear model. The logical purposes of intrigue can be found in Agalbjörn et al. (1997); Noori et al. (2011). The GT results can be organized by considering another term V-ratio, which restores a scaled invariant clamor evaluate in the vicinity of 0 and 1. The V-ratio is characterized as

$$V-ratio=\frac{\Gamma}{\sigma^{2}(y)} \tag{5}$$

where $\sigma^2(y)$ = variance of yield y, which provides a standardized measure of the Gamma statistic and empowers a judgment to be shaped, freely of the yield range, in the matter of how well the yield can be displayed by a smooth function. In looking at different yields, or yields from various informational collections, the V-ratio is a decent number to think about on the grounds that it is free of the yield range. A V-ratio close to zero demonstrates a high level of consistency (by a smooth model) of the specific yield. On the off chance that the V- ratio is near to one, the yield is identical to irregular commotion to the extent a smooth model is concerned.

## 2.3 M-test

Deciding the best possible length of the training data is imperative to enhance the prediction (Choubin and Malekian 2017). M-test curve is a method for deciding the quantity of input data required to create a stable asymptote. Here, we utilized M-test dependent on the V-ratio and gamma value to choose the best length of preparing and testing information in the neural network technique like some different works (e.g., Evans and Jones 2002; Remesan et al. 2008; Stefansson et al. 1997; Tsui et al. 2002; Noori et al. 2011). The values of V-ratio and gamma statistics are resolved with an expanding number of data points. Information length is resolved based on M-test curve stabilized for a particular value of V-ratio and gamma. This test decreases overfitting in nonlinear modelling (Shamim et al. 2016).

### 2.4 Artificial Neural Network

Artificial Neural Network (ANN) is a type of 'black box' model which is considered to be one of the computational tools for modeling nonlinear and complex phenomena without any preceding assumption through the processes involved. By adopting the past data, ANN can cultivate relatively accurate forecasting of the modelled parameters that may be used as a tool for replicating any physical phenomenon. In last two and half decade, ANN has gained wider stature among researchers working in the area of river flow modelling and other water resources problems (Kisi 2005; Choi and Cheong 2006; Cigizoglu and Kisi 2006; Kisi and Cigizoglu 2007; Zhu et al. 2007; Khuntia et al 2017). The most commonly used artificial neural network model is the multilayer perceptron feed forward (FF) technique and in which the back-propagation (BP) algorithm is frequently used for training these networks (Hornik 1989). The topology of FFBP ANNs consists of a set of neurons associated with links in a number of layers (Sahu et al. 2011). The basic unit of the network generally consists of an input layer, a hidden layer, and an output layer (Fig. 5). The input nodes draw the data values and transmit them to the hidden layer nodes. Each node of the hidden layers collects the inputs from all input nodes subsequently multiplying each input value by weight, attaches a bias to this sum, and passes on the results through a nonlinear transformation like sigmoid transform function. This forms the input either for the second hidden layer or the resulting transformed output from each output node is the network output. The critical step in building a robust ANN is to create an architecture, which should be as simple as conceivable and has a fast capacity for learning the dataset (Haykin 1994).

The flow in a non-prismatic compound channel is a fully complex hydraulic phenomenon, it was expected that the MLP model was not of a small size. To achieve an optimum structure for the MLP model, the size of the model is increased step by step. Different transfer functions including logsig (log-sigmoid transfer function), tansig (hyperbolic tangent sigmoid transfer function), purelin (linear transfer function) were tested. In other words, firstly, a model with one hidden layer involved eight (Mask a) or four (Mask b) neurons (equal to features of inputs) was considered. Then the transfer functions were tested. By choosing the proper transfer function in the next step was to improve the precision of the developed MLP model, the number of neurons and the hidden layer could be increased. Many theoretical and experimental works have shown that a single hidden layer is sufficient for ANNs to approximate any complex non-linear function (Cybenko, 1989; Jalili-Ghazizade and Noori et al., 2011). A major reason for this is that intermediate cells do not directly connect to output cells. Hence, they will have very small changes in their weight and learn very slowly (Gallant, 1993). This approach leads to achieving optimum structure and suitable performance in terms of computation cost.

Figure 5. Architecture of ANN model for discharge prediction with [8-10-1] network structure

## 2.5 Adaptive Neuro-Fuzzy Inference System (ANFIS)

The adaptive neuro-fuzzy inference system (FIS) is an artificial intelligence method, which is a sequence of the artificial neural network (ANN) and fuzzy system that uses the learning effectiveness of the ANN to evolve the fuzzy IF-THEN rules with proper membership functions derived from the training pair, whichever in turns lead to an inference. Such systems disregard the commitment of manual optimization of fuzzy system parameters and the tuning of the system parameters can be achieved by means of ANN. The merger of both ANN and FIS along these lines enhances framework execution without interceding of administrators. ANFIS is frequently used as a part of many water resources issues such as modeling of hydrological time series, reservoir operations, rainfall-runoff prediction and other related fields (Xu & Li, 2002; Unal et al. 2010; Yarar et al. 2009; Dorum et al. 2010).

Fig. 6. (a) A schematic diagram of ANFIS structure and (b) A schematic diagram of the fuzzy based inference system

The advantage of the approach is that one can utilize the ANFIS design to shape nonlinear functions to analyze nonlinear parameters yet to figure the desired outcome sensibly (Jang 1991, 1993, 1994). The goal of the present work is to anticipate flow in the converging and diverging compound channel which can be accomplished by adopting an innovative architecture of ANFIS structure. The structure can be constituted, a guideline for making an arrangement of fuzzy if-then principles and fuzzy inference frameworks accommodate membership functions to produce the result satisfactorily.

### *2.4.1 Architecture and basic learning rules*

ANFIS is a rule-based fuzzy rationale model that its principles perform throughout the training operation of the model. As shown in Fig. 6a, five layers are utilized to develop this inference structure. In this network structure, the input (layer 0) and yield (layer 5) hubs depict the sources of input and the yield, individually. In the hidden layers, there are a few fixed and adaptable hubs working as membership functions (MFs) and rules. To clarify the methodology of an ANFIS, we consider two information factors x, y, and one yield variable z. In the ANFIS model, the association among information and yield is communicated by the usage of if-then fuzzy rules. At that point, the model includes two fuzzy rules in perspective of Takagi and Sugeno's type (Sahu et al. 2011) and that can be expressed as follows:

Rule 1: If x is $A_1$ and y is $B_1$ then $z_1 = p_1 x + q_1 y + r_1$ (6)

Rule 2: If x is $A_2$ and y is $B_2$ then $z_2 = p_2 x + q_2 y + r_2$ (7)

where $A_1$, $B_1$, and $A_2$, $B_2$ are the semantic level, $p_1$, $q_1$, $r_1$ and $p_2$, $q_2$, $r_2$ are the ensuing parameters. If $z_1$ and $z_2$ are constants instead of linear equations, we have zero order TSK fuzzy-model. ANFIS structure consists of five number of layers (Fig. 6a). Different layers are described below: Layer 1 (Fuzzification layer) - Every node in this layer is a flexible node with a node function, Layer 2 (Rule layer) -Every node in this layer is a fixed node and acts as a basic multiplier, Layer 3 (Normalization layer)- In this layer, every node is an adaptive node marked as N. The $i^{th}$ node figures the proportion of the $i^{th}$ rule's terminating quality to the aggregate of all rules' terminating strengths, Layer 4 (Defuzzification layer) Every node in this layer is a flexible node with a function, Layer 5 (Output layer)- In this last layer, the single node is a settled node which processes the general yield as the entirety of every approaching signal. The purpose of the training algorithm for this design is to tune the over two parameter sets to make the ANFIS yield organizes the training information (Jang 1993; Sahu et al. 2011). Therefore, an adaptable framework is presented in Fig.

6a is practically proportionate to the fuzzy interface framework shown in Fig. 6b. From ANFIS design (Fig. 6a), it is observed that the given values of the premise parameters, the overall yield z can be imparted as a linear blend of the resulting parameters. In perspective of this observation, a hybrid learning standard is used here, which consolidates a back propagation technique and the least squares method to find a feasible of the forerunner and subsequent parameters (Jang 1991; Jang 1993). The particulars of the hybrid rule are given by Jang et al. (1997), where it is additionally asserted to be altogether quicker than the traditional back-propagation technique.

The primary confinement of the ANFIS model is related to the number of input parameters. On the off chance that ANFIS inputs surpass five, the computational time and rule numbers will increase, so ANFIS with grid partitioning won't have the capacity to show yield as for inputs. For our case, the quantities of information sources were eight and four, so grid partitioning and sub-clustering has been done respectively to generate FIS.



### *2.4.2 Grid partition (GP)*

This technique creates a Sugeno-type FIS structure from training datasets. GP isolates the input data into various nearby fuzzy locales utilizing a pivot paralleled partition in view of a predefined number of membership functions. GP strategy includes eight membership functions types (trimf, trapmf, chime MF, gaussmf, gauss2mf, if, dsigmf, psigmf). For mask [101110000] input combination, this method is adopted to produce FIS. The quantity of MFs can be indicated in a relationship with each information. Since this is a Sugeno-type, just a single yield can be utilized. The yield function can be constant or linear. The quantity of yield MFs is the same as the number of rules created by this technique. In this subsection, the elective models comprise of different FIS structures are produced by utilizing diverse MF features (types, numbers) for input membership function parameters.

### *2.4.3 Subtractive clustering (SC)*

The optimum number and form of fuzzy rules determination is the most crucial step, and various algorithms have been developed to automate this process, such as k-means clustering, fuzzy C-means clustering, and subtractive clustering (Jang 1993; Noori et al. 2011). When the number of input parameters is more than five then generally subtractive clustering technique is adopted which save run time process and take less computational space (Sahu et al. 2016). The subtractive clustering method assumes that each data point is a potential cluster center and calculates a measure of the likelihood that each data point would define the cluster center on the basis of the density of surrounding data points. The steps of the fuzzy-model algorithm can be summarized as follows: (1) it selects the data point with the highest potential to be the first cluster center (which is usually considered between 0.2 and 0.5); (2) it removes all data points in the vicinity of the first cluster center as determined by the range(radius) of influence (which is usually considered as 0.5); (3) iterate the process until all of the data fall within the radii of a cluster center (which is considered as 1.25, here). The vector options can be used for identifying clustering algorithm parameters to override the default values. These components of the vector options are specified as Range of influence (ROI), Squash factor (SF), Accept ratio (AR) and Reject ratio (RR). In perspective of the cluster data, a Sugeno-type FIS framework that best models the information conduct can be produced. The information clustering system used in this paper is subtractive clustering (Chopra et al. 2006) for input parameter more than five numbers. In light of the thickness of encompassing information focuses, it can appraise the number of clusters and the cluster centers in an arrangement of information. The fuzzy principles found by bunching information are more uniquely crafted to the input information; subsequently, the FIS will have much fewer rules than that without information clustering. This algorithm works like a pre-processor to ANFIS for deciding the basic rules. At the point when the FIS is created, four parameters for subtractive clustering should be determined (Chopra et al. 2006) which are mentioned below:

1) ROI-range of influence (default 0.5), to show the extent of the effect of a gathering center. The more neighboring information focuses a data point can encase, the higher potential it has as a cluster center;

2) SF-squash factor (default 1.25), multiplying $q_1$ to decide the area of a cluster center inside which the nearness of other bundle centers is discouraged;

3) AR-accept ratio (default 0.5), to set the potential above which another information point will be acknowledged as a cluster center;

4) RR-reject (default 0.15), to set the potential beneath which an information point will be dismissed as a cluster center.

## 3 Sources of Data and Influencing Flow Parameters

For this research work, we collected the 196 experimental data on converging and diverging compound channel along from the are published papers by Bousmar (2002); Bousmar et al. (2006); Rezaei (2006); Yonesi et al. (2013) and Naik and Khatua (2016) are presented in Table 1.

Table 1. Details of geometric, hydraulic and surface parameters for all types of channel collected from published data on diverging and converging compound channel

Table 2. Statistical characteristics of the data under consideration

From extensive literature survey on compound channels, it is seen that the investigators such as Knight and Demetriou (1983); Yang (2005); Parsaei et al. (2017); Khuntia et al. (2018) have suggested that flow in compound channel depends on friction factor ratio, area ratio, width ratio, hydraulic radius ratio, relative flow depth, flow aspect ratio and bed slope. Das et al. (2016) proved the dependency of energy loss and discharge on diverging/converging angles and relative longitudinal distance for non-prismatic geometry. Hence, in the present study, for the development of ANN and ANFIS model, nine non-dimensional input parameters, which influence the flow quantity at a different section of non-prismatic reach have been considered. The details about these non-dimensional parameters are described below:

Friction factor ratio ($Fr$) is the ratio of main channel friction factor $f_{mc}$ to floodplain $f_{fp}$, area ratio ($A_r$) is the ratio of main channel area to floodplain area, hydraulic radius ratio ($Rr$) is the hydraulic radius of the main channel to that of floodplain, flow aspect ratio ($\delta^*$) is the ratio of the width of the main channel to the depth of flow over main channel, width ratio ($\alpha$) is the ratio of width of floodplain ($B$) to width of the main channel ($b$), Relative flow depth ($\beta$) = $(H-h)/H$. where $H$ - height of water at a particular section and, $h$ - bank full depth or main channel depth, Relative longitudinal distance ($X_r$=$l/L$) from a reference or origin is the ratio of the distance ($l$) of the arbitrary reach or section in longitudinal direction of the channel to the total length ($L$) of the non-prismatic channel, converging or diverging angle ($\theta$) - angle of floodplain to the main channel, it is taken as positive for diverging angle and negative for converging angle, longitudinal slope ($S_0$) - bed slope of the channel. The statistical characteristics of the data under consideration are presented in Table 2. Table 3 shows the error indices in discharge prediction. evaluated by analytical approaches

Total nine flow variables were chosen as input parameters and flow as an output parameter. The dependency flow ($Q$) on these aforementioned parameters can be written in a functional relationship as

$$Q = f\left(f_r, A_r, R_r, \beta, S_0, \delta^*, \alpha, \theta, X_r\right) \quad (8)$$

Table 3. Error indices result of the analytical approaches

## 4. Model input selection and training data length

In practice, the Gamma (Γ) test can be accomplished by utilizing the winGamma software (Durrant 2001). The authors believe that this methodology is very effective and could be used as a part of various hydraulic nonlinear modelling endeavors. Gamma Test is used to measure uncertainty by Γ value and V-ratio. This paper shows all blends of information data that influence the flow in a different section of the non-prismatic compound channel by using full embedding. A full embedding tries for each blend of contributions to make sense of which blend yields the smallest absolute Γ value. It returns the number of results asked. In case there are 'm' scalar sources of information, by then there are 2m-1 vital blends of data sources (nine in this investigation). The best one of these assorted blends can be controlled by watching that with the minimum Γ value, which demonstrates a measure of the best MSE. Subsequently, we played out the GT in different estimations by changing the number of contributions to the model and minimum estimation of Γ was observed when we used every fourth contribution for all four input value. V-ratio is the measure of predictability of given yields using accessible data sources. An input dataset with a low value of MSE and V-ratio is considered as the best situation for the modelling. 400 examinations have been made in winGamma software for nine to three representative blends of non-dimensional parameters but in this paper, 20 different blends (including the best one), are orchestrated in Table 4. From Table 4 we can determine that the blend of 8 parameters with mask [111111110] and 4 parameters with mask [101110000] can make a decent model in contrast with other conceivable blends. For the later mask Γ, the V-ratio value is observed to be superior to the former mask.

Deciding the best possible length of the training data is imperative to enhance the prediction (Choubin and Malekian 2017) through ANN or ANFIS model. In winGamma software, M-test curve is a method for deciding the quantity of information required to create a stable asymptote. Here, we utilized M-test in light of the V-ratio and Γ value to choose the best length of training and testing information in the neural network technique similar to some others work (e.g., Evans and Jones 2002; Remesan et al. 2008; Tsui et al. 2002; Noori et al. 2011). The estimations of V-proportion and Γ insights are determined by expanding the number of data points. Data length is resolved in view of M-test curve stabilized for a particular value of V-ratio and Γ value (Shamim et al. 2016; Choubin and Malekian 2017). The M test curves for masks [111111110] and [101110000] are shown in Figs. 6a and 6b respectively. Figure 7 demonstrates that a training information length of 154 and 167 is adequate respectively for 8 and 4 input parameters blend in the Gamma statistics to wind up noticeably steady and low.



Fig. 7. M-test curve: the variation of gamma statistic and V-ratio with unique data points to determine the proper length of training data for mask a) [111111110] and b) [101110000]

Table 4. Determining the best combination for flow ($Q$) in non-prismatic compound channel

## 5. Development of Models for Discharge Prediction

To develop ANN and ANFIS models, the input and output data were mapped into the domain [0.05,0.95] utilizing the Equation (9), because the best range suggested for normalization is in the vicinity of 0.05 and 0.95 (Hsu et al. 1995). This would increase the accuracy and speed of ANN and ANFIS performance.

$$a_{norm} = 0.05 + 0.90\frac{(a - a_{\min})}{(a_{\max} - a_{\min})} \quad (9)$$

where $a_{norm}$ and $a$ are the normalized and original inputs; $a_{min}$, and $a_{max}$ indicate minimum and maximum of the input ranges, respectively.

The information to be utilized for training ought to be adequately large to cover the conceivable known variations in the problem domain (Kim and Valdes, 2003). From the M test, for the input blend of [111111110] mask ( i.e., mask-a), the total 196 data were divided into a training set 154 and testing set 42 and for [101110000] mask (i.e., mask-b), the training and testing set are 167 and 29 respectively. These fixed training and testing data length have been considered in both ANN and ANFIS to develop the robust discharge predictive model.

### 5.1 Artificial Neural Network model

In this approach, a multi-layer perceptron (MLP) feed forward back propagation (FFBP) network has been developed for both mask-a and mask-b. Tan-sigmoid function (tan) has been taken as a nonlinear activation function for the hidden layer, and linear transfer function (pure) for the output layer for both of the case (Noori et al 2011; Parsaei et al 2017). Figure 5 shows the schematic diagram of a feed-forward MLP with one hidden layer with ten neurons to estimate the discharge.

For the training of the FFBP network, the Levenberg-Marquardt (LM) method has been used because of the faster training process and occupy less memory in the system (Yazdi and Bardi 2011). Training and validating data sets are generally known as the calibration set. To compute the number of hidden neurons, an initial random number was employed. Afterward, the optimum number of hidden neurons was found to be found out by a trial and error procedure. For this around 250 simulations have been performed to get the best training and testing results for discharge prediction. The details of the best training parameter of ANN model for mask-a and mask-b is presented in Table 5.

Table 5. Different training parameters used for neural network analysis



### 5.2. Artificial Neuro Fuzzy Inference System model

To run a fuzzy model two alternatives are available, which includes subtractive fuzzy clustering (requiring less computational effort) and grid partitioning (requiring more computational effort). In this work, for eight inputs parameters, subtractive clustering and for four input parameters, the grid partitioning has been utilized as specified before. In subtractive clustering different trials have been made to get optimum value for ROI (0.52), SF (1.2), AR (0.5) and RR (0.15) for the 8 input parameters blend. The errors for subtractive clustering are shown in Table 6. Similarly, in grid partitioning for 4 input parameters, different MFs are chosen for each input parameter from 2 to 4 numbers with various MF types and the best optimal outcomes are presented in Table 6.

Table 6 Details of the best ANFIS model performance

## 6 Results and Discussions

The analytical approaches, ANN and ANFIS model were surveyed by the data gathered summarized in Table 1. The precision of the analytical approaches, ANN and ANFIS model have been evaluated by ascertaining the statistical error indices, for example, the coefficient of determination ($R^2$), mean absolute percentage error (MAPE), mean absolute error (MAE), root mean square error (RMSE), Nash-Sutcliff coefficient (E). The definitions of various errors are explained in (Das and Khatua 2018). It is noticeable that these indices are shown in Tables 3 and 6, present the value for the average error and not give any data about error distribution, so in addition to ascertaining the error indices, the execution of them are shown in Figs. 8-11 between the observed values and predicted values.

### 6.1 Analysis of analytical approaches

The strength of the traditional methods was assessed for ascertaining the flow in the non-prismatic compound open channel by utilizing the gathered datasets. The outputs of traditional methods are presented in Fig. 4. To know more about the strengths of the traditional methods, other specified statistical errors analysis was ascertained and exhibited in Table 3. With respect to Table 3, the $DCM_{v-i}$ is the most correct among the different approaches and has an appropriate accuracy by the coefficient of determination of 0.74. The appropriate accuracy of this technique is identified with separating the compound open channel cross segment as a main channel and floodplains and considering the idea of the mass and force in the method development process. As appeared in Fig. 4, for given actual discharge there is a huge variation in predicted results. This is because, for a single discharge value in converging and diverging compound channels, the flow is calculated at different sections of the non-prismatic portion using common formula. The present analytical approaches which are providing some good results for prismatic compound channel segments does not include the concept of mass and momentum exchange between main channel and floodplains for non-prismatic geometry (Bousmar et al. 2006). Table 4 demonstrates that the poorest execution is identified with the SCM by correlation of around 47%, and it is seen from Fig. 4 that, by increasing the discharge, the performance of this technique for a various segment of non-prismatic compound channel quickly decreases. The fundamental explanation behind the infirmity of SCM is identified with ignoring the energy exchanging between the main channel and floodplains. IDCM and EDM also provide discharge values with MAPE of 35% and 33% respectively for non-sections. For a given discharge, at converging and diverging compound channels, the predicted values evaluated by analytical approaches are overestimated and underestimated for most of the sections. Because the flow is non-uniform from section to section and the presented analytical model does not consider any parameter which can manage the non-uniformity of flow.

### 6.2 Analysis using the ANN and ANFIS model

In this work, distinctive blends of information (non-dimensional datasets) are investigated to evaluate their effect on flow modelling (Table 5). The ANN and ANFIS model have been created and tried for anticipating flow in the non-prismatic compound channel. The two non-dimensional parameters blends are chosen from the Gamma test, mask a (incorporates $F_r$, $Ar$, $Rr$, $\beta$, $S0$, $\delta^*$, $\alpha$, $X_r$) and mask-b (incorporates $F_r$, $Rr$, $\beta$, $S_0$). The amount of information required to foresee the alluring yield was analyzed utilizing the M-Test with different information lengths for two blends. This demonstrates that a training data length of 154 and 167 is adequate for the $\Gamma$ statistics respectively for mask-a and mask-b blends to become stable and low. Measurable aftereffects of various blends are presented in Table 4. From Table 4, it is noticed that from 9 non-dimensional input parameters, converging and diverging angle i.e., $\theta$ isn't significant in anticipating discharge from section to section. This is on account of our goal to predict the discharge that crosses a specific section. For a given $\theta$, there are different sections can be found and the sectional geometry can be taken care of by $Ar$ or $Rr$, so the $\theta$ value is redundant in demonstrating flow in non-prismatic compound channels.

Figures 8 and 9 show the results of model calibration and testing stages against observed data from the best-trained ANN model. The figure indicates that the predicted values of discharge generally have a good agreement with the observed data. On the other hand, it shows that the extreme discharge values obtained from the ANN model do not correspond to the observed ones. There was a significant difference between the predicted and observed extreme values. Therefore, although the ANN model generally produces an acceptable performance in predicting discharge in the non-prismatic compound channel, it is not capable of predicting the extreme values accurately. ANN model found to provide MAPE value of 16.3% and 13.2% respectively for mask –a and mask –b respectively.



Fig. 8 Predicted and observed data for calibration step of ANN model a) for 8 input parameters and b) for 4 input parameters

Fig. 9 Predicted and observed data for testing step of ANN model a) for 8 input parameters and b) for 4 input parameters

For simulation with the ANFIS model, a FIS structure from information utilizing subtractive clustering for mask-a and grid portioning for mask-b have been produced. In subtractive clustering (SC) technique for grid generation, different parameters are enhanced to get best outcomes as demonstrated in Table 6. The execution of the ANFIS demonstrates utilizing SC strategy amid the training and testing stages appears in Figs. 10 (a) and 11 (a). In grid partition (GP) technique of grid generation, the utility of different MFs, for example, generalized bell shape MF (gbellmf), Gaussian curve MF(gaussmf), and triangular-shaped MF (trimf) were tested. Amid the development, ANFIS model found that the gaussmf has a superior performance in contrast with others. The structure of the ANFIS demonstrates which had the best performance is presented in Table 6. The Gaussian function (gaussmf) was considered for the MF with 4 numbers and the weighted average (wtaver) approach was considered for the defuzzification technique. Allocating of the MFs to the info parameters, depending on the trial and error procedure (Sahu et al. 2012). The execution of the ANFIS model amid the preparation and testing stages is shown in the Figs. 10 (b) and 11 (b).



Fig. 10 Predicted and observed data for calibration step of ANFIS model a) for 8 input parameters and b) for 4 input parameters

Fig. 11 Predicted and observed data for testing step of ANFIS model a) for 8 input parameters and b) for 4 input parameters

The results of the computation of the error indices for the ANFIS model are shown in Table 6. From Table 6, for the SC method, the R-value of the ANFIS model amid the preparation and testing stage are 0.99 and 0.82, respectively. For the GP method, the $R^2$ esteem is observed to be 0.98 and 0.86 for preparing and testing stage respectively. The ANFIS model structure affirms the results of the ANN modelling the flow in the compound open channel. MAPE esteem for SC-ANFIS model and GP-ANFIS model is observed to be 16.3% and 9.4% which demonstrates that

SC demonstrates which incorporates eight non-dimensional info parameters indicates poor outcomes contrasted with GP strategy containing four input parameters. This is due to of the modelling of flow by considering parameters like $F_r$, $Rr$, $\beta$, and $S_0$ is significant, contrasting with the including of other four more input parameters like $Ar$, $\delta*$, $\alpha$ and $Xr$ to it as it clarified in gamma test. For mask-a, eight input parameters in the gamma test give the gamma value as - 0.001 and V-value as - 0.007 while four input parameters named as mask-b gives 0.0002 and 0.001 which is very close to zero. Additionally, to evaluate the performance of the ANN and ANFIS model, observed discharge values are plotted against the predicted ones (SC model for mask-a and GP model for mask-b) in Figs. 12 and 13 for testing stage information respectively. In Fig. 12 for both the mask the $R^2$ value found to be less than 0.85. Figure 13 indicates that the GP model for mask 10111000 demonstrates the high value of the coefficient of determination which implies the ANFIS model with four non-dimensional parameters like $F_r$, $Rr$, $\beta$, and $S_0$ gives a better model to predict discharge in converging and diverging compound channels.

Fig. 12 Comparison between the ANN model predicted value and observed value of discharge

Fig. 13 Comparison between the ANFIS model predicted value and the observed value of discharge

ANN and ANFIS model both are able to predict the discharge with more than 80% accuracy but due to less number of data set (196 data) consider in this study, the learning ability of training parameters is faster in ANFIS. The number of simulations to get best training and testing results are much more than ANFIS simulation trials. ANN has a problem of overt-training, it has been observed that by increasing the number hidden layers, there are no significant changes in the results. ANN model provides higher error in terms of MAPE in comparison GP technique adopted in ANFIS modelling.

## 7. Conclusions

In this investigation, some well-known scientific methodologies for computing the flow in the non-prismatic compound open channel were surveyed. For this reason, 196, exploratory data on a non-prismatic compound channel which were found from some reputed journal were collected. The results of the error indices for the output of analytical approaches showed that the performance of $DCM_{v-i}$ by the coefficient of determination of about 0.73 has acceptable performance for evaluating the flow in converging and diverging compound open channels. To accomplish more noteworthy exactness in the flow computation, the ANN and ANFIS soft-computing techniques are prepared based on the same data collected. Gamma test and M test has been performed to choose the most significant non-dimensional info parameters blends for modelling the discharge. The following results have been achieved in the present investigation:

- Gamma test reveals that for the present study, the friction factor proportion, relative flow depth, relative hydraulic radius and bed slope are the most critical parameter to predict the discharge in non-prismatic compound channel over the other non-dimensional parameters, such as, area ratio, width ration, flow aspect ratio, relative longitudinal distance and converging or diverging angles.
- Two models in ANFIS has been tried where for FIS generation, subtractive grouping for eight input parameters and grid partition for four input parameters has been performed. Ascertaining the errors for the ANFIS results demonstrated that the performance of the ANFIS

model utilizing 4 non-dimensional information parameters give an $R^2$-value of 0.96 and 0.86 for training and testing stages respectively is so appropriate for modelling the flow of converging and diverging compound channels.

- Converging or diverging angle is observed to be insignificant to predict the discharge at various section of the non-prismatic compound channels as it has been taken care by relative hydraulic radius.

- Comparison of the performance of the ANFIS model with ANN and analytical approaches demonstrated that the ANFIS model is more precise as it is evident from the error indices.

## APPENDIX



Appendix 1. All nine input variables data of converging and diverging compound channel collected

## NOMENCLATURE

| | |
|---|---|
| $Q_{fp}$ | Discharges carried by the floodplain |
| $Q$ | Measured discharge |
| $Q_{mc}$ | Discharges carried by the main channel |
| $R_{fp}$ | Hydraulic radius of floodplain |
| $R_{mc}$ | Hydraulic radius of main channel |
| $S_0$ | Bed slope of channel |
| $R_r$ | Relative hydraulic radius |
| $f$ | Darcy's friction factors |
| $n$ | Manning's roughness coefficient |

| | |
|---|---|
| $b$ | Main channel bottom width |
| $H$ | Total flow depth over main channel |
| $h$ | Bank full depth |
| $P$ | Wetted perimeter |
| $R$ | Hydraulic radius |
| $A$ | Area of the compound channel |
| $B$ | Total width of compound channel |
| E | Nash-Sutcliff coefficient |
| $Q$ | Discharges carried by the whole channel |
| $T$ | Top width of compound section |
| $U$ | Local stream wise velocity |
| $f_r$ | Relative friction factor |
| $A_r$ | Area ratio |
| $X_r$ | Relative longitudinal distance |
| $g$ | Gravitational acceleration |
| $\alpha$ | Width ratio |
| $\beta$ | Relative flow depth |
| $\delta^*$ | Flow aspect ratio of main channel |
| $\theta$ | Diverging or converging angle |
| $R^2$ | Coefficient of Determination |
| $\rho$ | Density of water |
| $q^g$ | Geometrical exchange discharge |

$q^t$ Turbulence exchange discharge

**Abbreviations**

| | |
|---|---|
| DCM | Divided Channel Method |
| EDM | Exchange Discharge Model |
| IDCM | Interacting Divide channel method |
| MAPE | Mean Absolute Percentage Error |
| RMSE | Root Mean Square Error |
| SCM | Single Channel Method |
| FIS | Fuzzy Inference System |



## References

Agalbjorn, S., Koncar, N., Jones, A.J., 1997. A note on the gamma test. Neural Computing Applied 5, 131–133.

Al-Khatib, I. A., Dweik, A. A., & Gogus, M. 2012. Evaluation of separate channel methods for discharge computation in asymmetric compound channels. Flow Measurement and Instrumentation, 24, 19-25.

Atabay, S., & Knight, D. W. 2006. 1-D modelling of conveyance, boundary shear and sediment transport in overbank flow. Journal of Hydraulic Research, 44(6), 739-754.

Bousmar, D. 2002. Flow modelling in compound channels (Doctoral dissertation, Birmingham University).

Bousmar, D., & Zech, Y. 1999. Momentum transfer for practical flow computation in compound channels. Journal of hydraulic engineering, 125(7), 696-706.

Bousmar, D., Proust, S., & Zech, Y. 2006. Experiments on the flow in an enlarging compound channel. In River Flow 2006: Proceedings of the International Conference on Fluvial Hydraulics, Lisbon, Portugal, 6–8 September 2006 (pp. 323-332).

Brunner, G. W. 2002. Hec-ras (river analysis system). In North American Water and Environment Congress & Destructive Water (pp. 3782-3787). ASCE.

Chlebek, J. 2009. “Modelling of simple prismatic channels with varying roughness using the SKM and a study of flows in smooth non-prismatic channels with skewed floodplains.” Doctoral dissertation, University of Birmingham.

Chopra, S., Mitra, R. and Kumar, V. 2006 Analysis of Fuzzy PI and PD Type Controllers Using Subtractive Clustering. International Journal of Computational Cognition, 4, 30-34.

Choubin, B., & Malekian, A. 2017. Combined gamma and M-test-based ANN and ARIMA models for groundwater fluctuation forecasting in semiarid regions. Environmental Earth Sciences, 76(15), 538.

Das B.S., Khatua K. K., Devi K. 2016. Prediction of energy loss in compound channels having enlarging floodplains. In River Flow- 2016 (pp. 65-71). CRC Press.

Das, B. S., & Khatua, K. K. 2018. Flow resistance in a compound channel with diverging and converging floodplains. Journal of Hydraulic Engineering, 144(8), 04018051.

Devi, K., Khatua, K. K., and Das, B. S. 2016. A numerical solution for depth-averaged velocity distribution in an open channel flow. ISH Journal of Hydraulic Engineering, 22 (3): 262–271

Dorum, A., Yarar, A., Sevimli, M. F., & Onüçyildiz, M. 2010. Modelling the rainfall–runoff data of susurluk basin. Expert Systems with Applications, 37(9), 6587-6593.

Durrant, P.J., 2001. winGamma: a non-linear data analysis and modeling tool with applications to flood prediction. Ph.D. thesis, Department of Computer Science, Cardiff University, Wales, UK.

Evans, D., & Jones, A. J. 2002. A proof of the Gamma test. In Proceedings of the Royal Society of London A: Mathematical, Physical and Engineering Sciences (Vol. 458, No. 2027, pp. 2759-2799). The Royal Society.

Han, D., Yan, W., & Nia, A. M. 2010, July. Uncertainty with the Gamma Test for model input data selection. In Neural Networks (IJCNN), The 2010 International Joint Conference on (pp. 1-5). IEEE.

Hsu, K. L., Gupta, H. V., & Sorooshian, S. 1995. Artificial neural network modeling of the rainfall-runoff process. Water resources research, 31(10), 2517-2530.

Huthoff, F., Roos, P. C., Augustijn, D. C., & Hulscher, S. J. 2008. Interacting divided channel method for compound channel flow. Journal of hydraulic engineering, 134(8), 1158-1165.

James, M. & Brown, B.J. 1977. Geometric parameters that influence floodplain flow, Report WES-RR-H-77-1, USACE, Vicksburg, USA.

Jang, J. S. R., Sun, C. T., & Mizutani, E. 1997. Neuro-fuzzy and soft computing: A computational approach to learning and machine intelligence. London: Prentice- Hall International.

Jang, R. J. 1991. Fuzzy modeling using generalized neural networks and Kalmman filter algorithm. In Proceedings of the ninth national conference on artificial intelligence (pp. 762–767).

Jang, R. J. 1993. ANFIS: Adaptive-network-based fuzzy inference system. IEEE Transaction on Systems of Max and Cybernetics, 23(03), 665–685.

Jang, R. J. 1994. Structure determination in fuzzy modeling: A fuzzy CART approach. In Proceedings of IEEE International conference on fuzzy systems, Orlando, Florida.

Khuntia, J. R., Devi, K., & Khatua, K. K. 2018. Boundary shear stress distribution in straight compound channel flow using artificial neural network. Journal of Hydrologic Engineering, 23(5), 04018014.

Kim, T.W., Valdes, J.B., 2003. Nonlinear model for drought forecasting based on a conjunction of wavelet transforms and neural networks. Journal of Hydrologic Engineering 6, 319–328.

Knight, D. W., & Demetriou, J. D. 1983. Floodplain and main channel flow interaction. Journal of Hydraulic Engineering, 109(8), 1073-1092.

Knight, D. W., Shiono, K., & Pirt, J. 1989. Prediction of depth mean velocity and discharge in natural rivers with overbank flow. In Proceedings of the International Conference on

Hydraulic and Environmental Modelling of Coastal, Estuarine and River Waters (pp. 419-428). Gower Publishing

Lotter, G. K. 1933. Considerations on hydraulic design of channels with different roughness of walls. Transactions, All-Union Scientific Research Institute of Hydraulic Engineering, Leningrad, 9, 238-241.

Naik, B., & Khatua, K. K. 2016. Boundary shear stress distribution for a converging compound channel. ISH Journal of Hydraulic Engineering, 22(2), 212-219.

Noori, R., et al. 2011. "Assessment of input variables determination on the SVM model performance using PCA, gamma test, and forward selection techniques for monthly streamflow prediction." J. Hydrol., 401(3), 177–189.

Parsaie, A., Yonesi, H., & Najafian, S. 2017. Prediction of flow discharge in compound open channels using adaptive neuro-fuzzy inference system method. Flow Measurement and Instrumentation, 54, 288-297.

Proust, S. 2005. "Ecoulements non-uniformes en lits composés: effes de variations de largeur du lit majeur." Doctoral dissertation, INSA de Lyon.

Proust, S., Bousmar, D., Rivière, N., Paquier, A., & Zech, Y. 2010. Energy losses in compound open channels. Advances in water Resources, 33(1), 1-16.

Remesan, R., Shamim, M. A., & Han, D. 2008. Model data selection using gamma test for daily solar radiation estimation. Hydrological Processes, 22(21), 4301-4309.

Rezaei, B. 2006. Overbank flow in compound channels with prismatic and non-prismatic floodplains (Doctoral dissertation, University of Birmingham).

Sahu, M., Khatua, K. K., & Mahapatra, S. S. 2011. A neural network approach for prediction of discharge in straight compound open channel flow. Flow Measurement and Instrumentation, 22(5), 438-446.

Sellin, R. H. J. 1964. A laboratory investigation into the interaction between the flow in the channel of a river and that over its floodplain. La Houille Blanche, (7), 793-802.

Shamim, M. A., Hassan, M., Ahmad, S., & Zeeshan, M. 2016. A comparison of Artificial Neural Networks (ANN) and Local Linear Regression (LLR) techniques for predicting monthly reservoir levels. KSCE Journal of Civil Engineering, 20(2), 971-977.

Shiono, K., Al-Romaih, J. S., & Knight, D. W. 1999. "Stage-discharge assessment in compound meandering channels." Journal of Hydraulic Engineering, 125(1), 66-77.

Stefansson, A., Končar, N., & Jones, A. J. 1997. A note on the gamma test. Neural Computing & Applications, 5(3), 131-133.

Tsui, A.P.M., Jones, A.J., deOliveira, A.G., 2002. The construction of smooth models using irregular embeddings determined by a gamma test analysis. Neural Computing Applied 10, 318–329.

Unal, B., Mamak, M., Seckin, G., & Cobaner, M. 2010. Comparison of an ANN approach with 1-D and 2-D methods for estimating discharge capacity of straight compound channels. Advances in engineering software, 41(2), 120-129.

Vafakhah, M. 2012. Application of artificial neural networks and adaptive neuro-fuzzy inference system models to short-term streamflow forecasting. Canadian Journal of Civil Engineering, 39(4), 402-414.

Wormleaton, Peter R., John Allen, and Panos Hadjipanos 1982. "Discharge assessment in compound channel flow." Journal of the Hydraulics Division 108, no. 9: 975-994.

Xu, Z. X., & Li, J. Y. 2002. Short-term inflow forecasting using an artificial neural network model. Hydrological Processes, 16(12), 2423-2439.

Yang, K., Cao, S., & Liu, X. 2005. Study on resistance coefficient in compound channels. Acta Mechanica Sinica, 21(4), 353-361.

Yarar, A., Onucyıldız, M., & Copty, N. K. 2009. Modelling level change in lakes using neuro-fuzzy and artificial neural networks. Journal of Hydrology, 365(3-4), 329-334.

Yonesi, H. A., Omid, M. H., & Ayyoubzadeh, S. A. 2013. The hydraulics of flow in non-prismatic compound channels. J Civil Eng Urban, 3(6), 342-356.

Zahiri, A., & Dehghani, A. A. 2009. Flow discharge determination in straight compound channels using ANN. World Academy of Science, Engineering and Technology, 58, 12-15.

Figure 1. Schematic diagram of non-prismatic compound channel, (a) Converging compound channel ($\theta$=3.81°), (Rezaei 2006) and (b) Diverging compound channel ($\theta$=3.81°), (Yonesi et al. 2013)

Figure 2. Kinds of isolating limit between the main channel and floodplains. (Parsaei et al., 2017)

Figure 3. Flow chart of methodology used to develop a discharge predictive model

Figure 4. Correlation between the result of analytical approaches versus the measured discharge

Figure 5: Architecture of ANN model for discharge prediction with [8-10-1] network structure

Figure 6. (a) A schematic diagram of ANFIS structure and (b) A schematic diagram of fuzzy based inference system

Figure 7. M-test curve: the variation of gamma statistic and V-ratio with unique data points to determining the proper length of training data for mask a) [111111110] and b) [101110000]



Figure 8. Predicted and observed data for calibration step of ANN model

Figure 9. Predicted and observed data for testing step of ANN model

Figure 10. Predicted and observed data for calibration step of ANFIS model

Figure 11. Predicted and observed value for testing step of ANFIS model

Figure 12. Comparison between the ANN model predicted value and observed value of discharge

Figure 13. Comparison between the ANFIS model predicted value and observed value of discharge

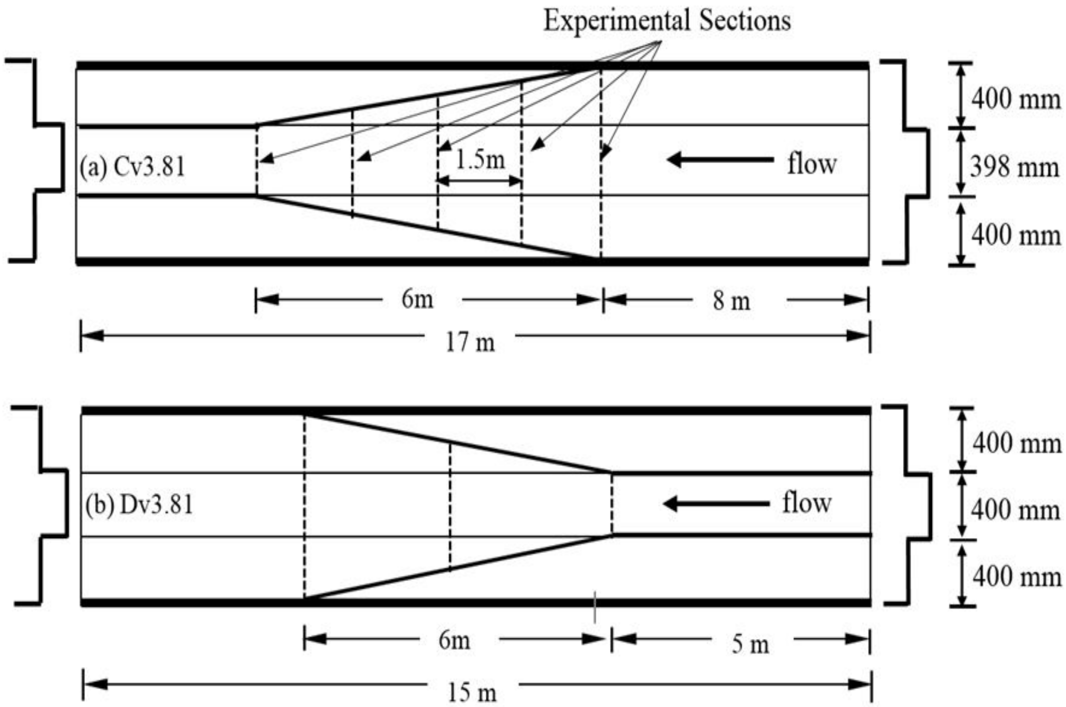


Figure 1. Schematic diagram of non-prismatic compound channel, (a) Converging compound channel ($\theta$=3.81°), (Rezaei 2006) and (b) Diverging compound channel ($\theta$=3.81°), (Yonesi et al. 2013)

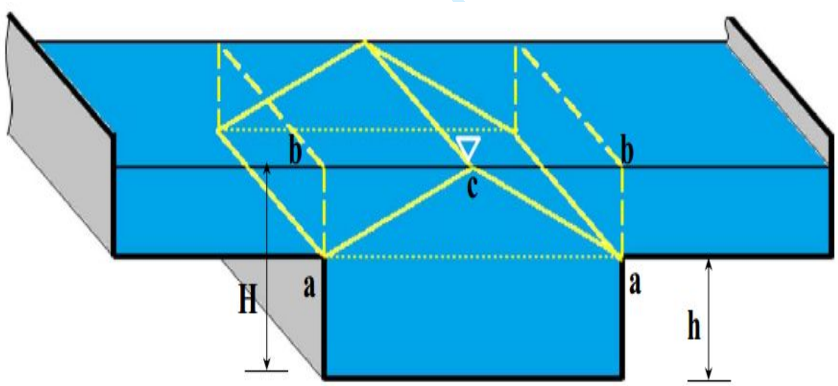


Figure 2. Kinds of isolating limit between the main channel and floodplains. (Parsaei, 2016)

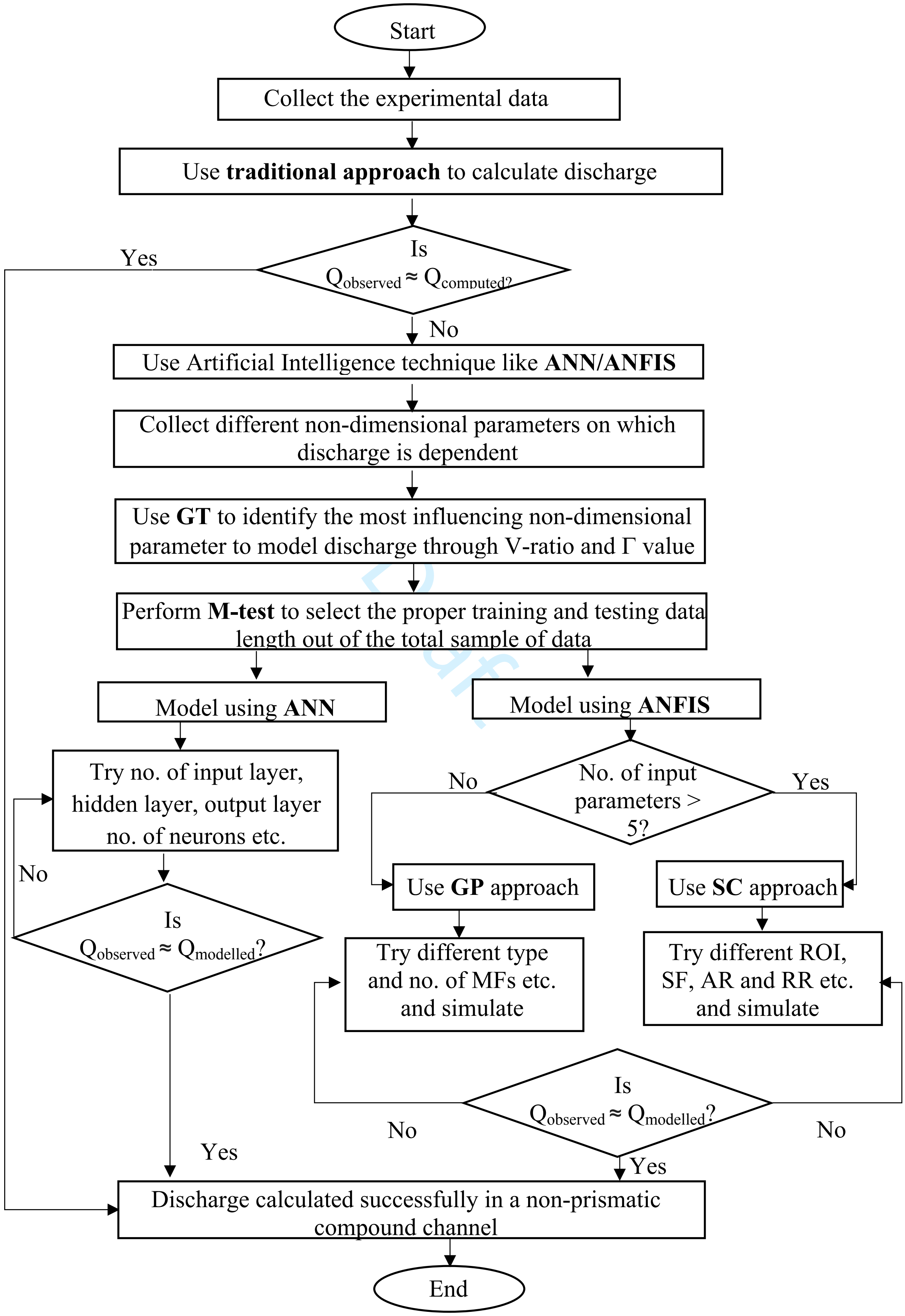


Figure 3. Flow chart of methodology used to develop a discharge predictive model

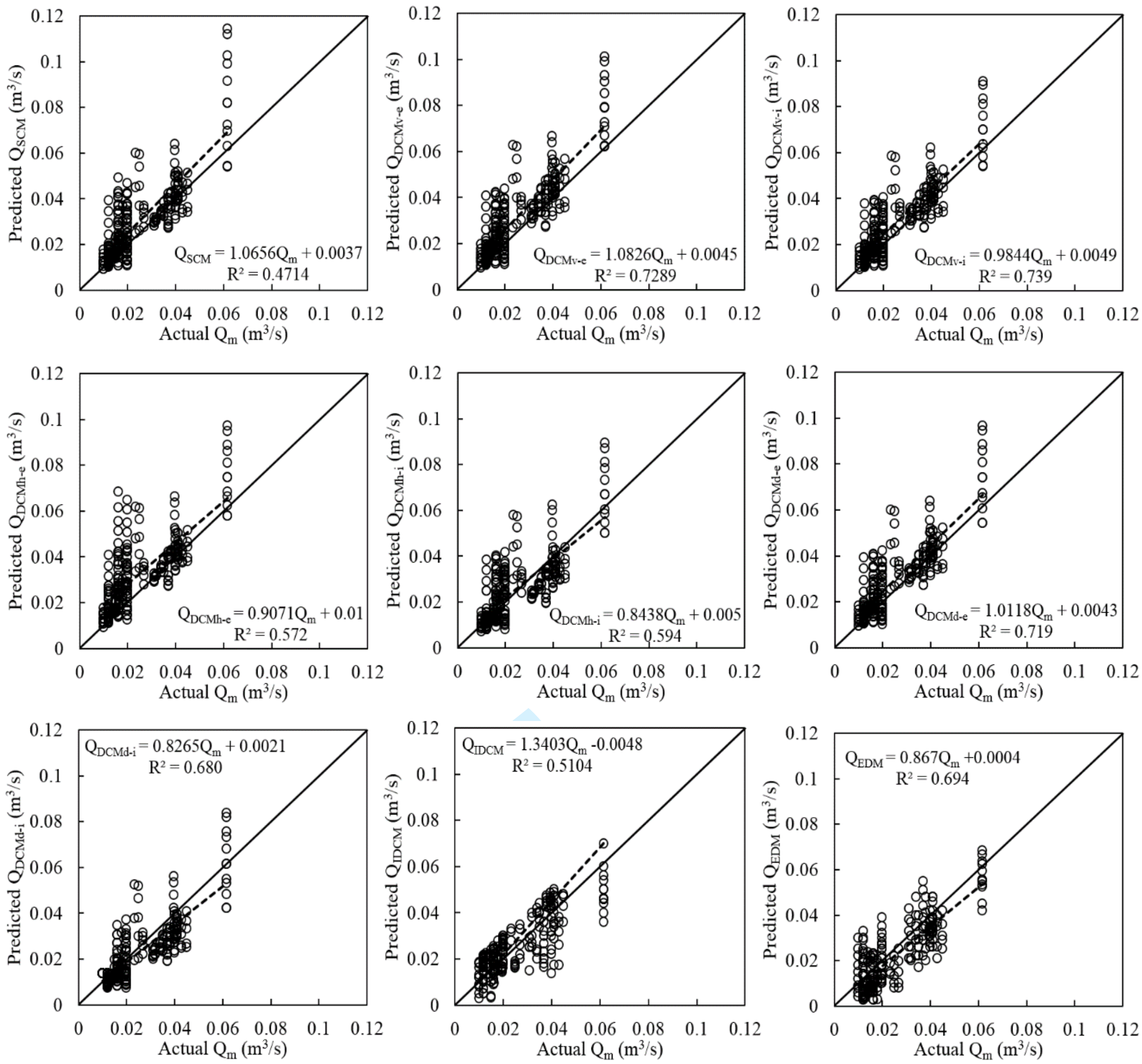


Figure 4. Correlation between the result of analytical approaches versus the measured discharge

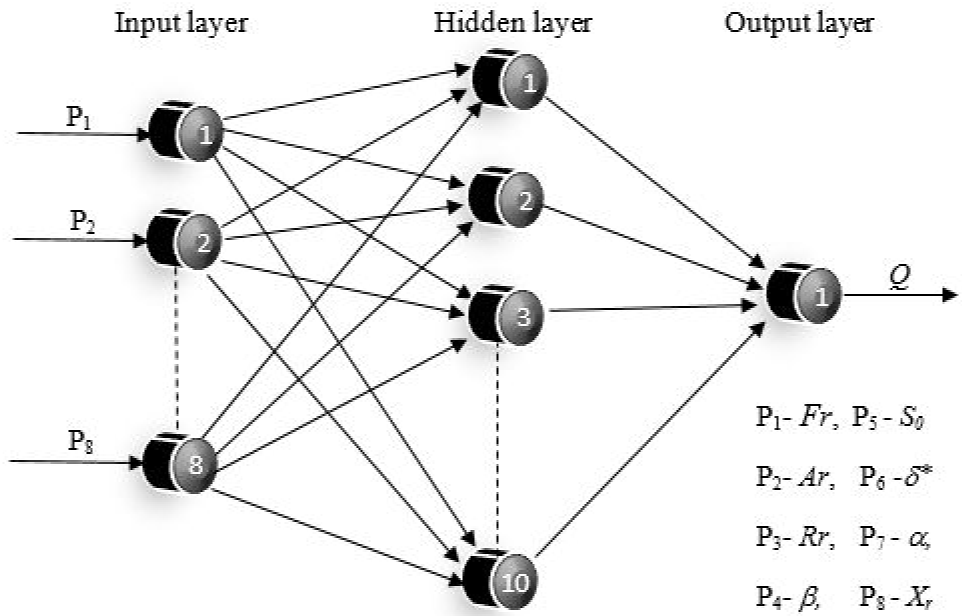


Figure 5: Architecture of ANN model for discharge prediction with [8-10-1] network structure

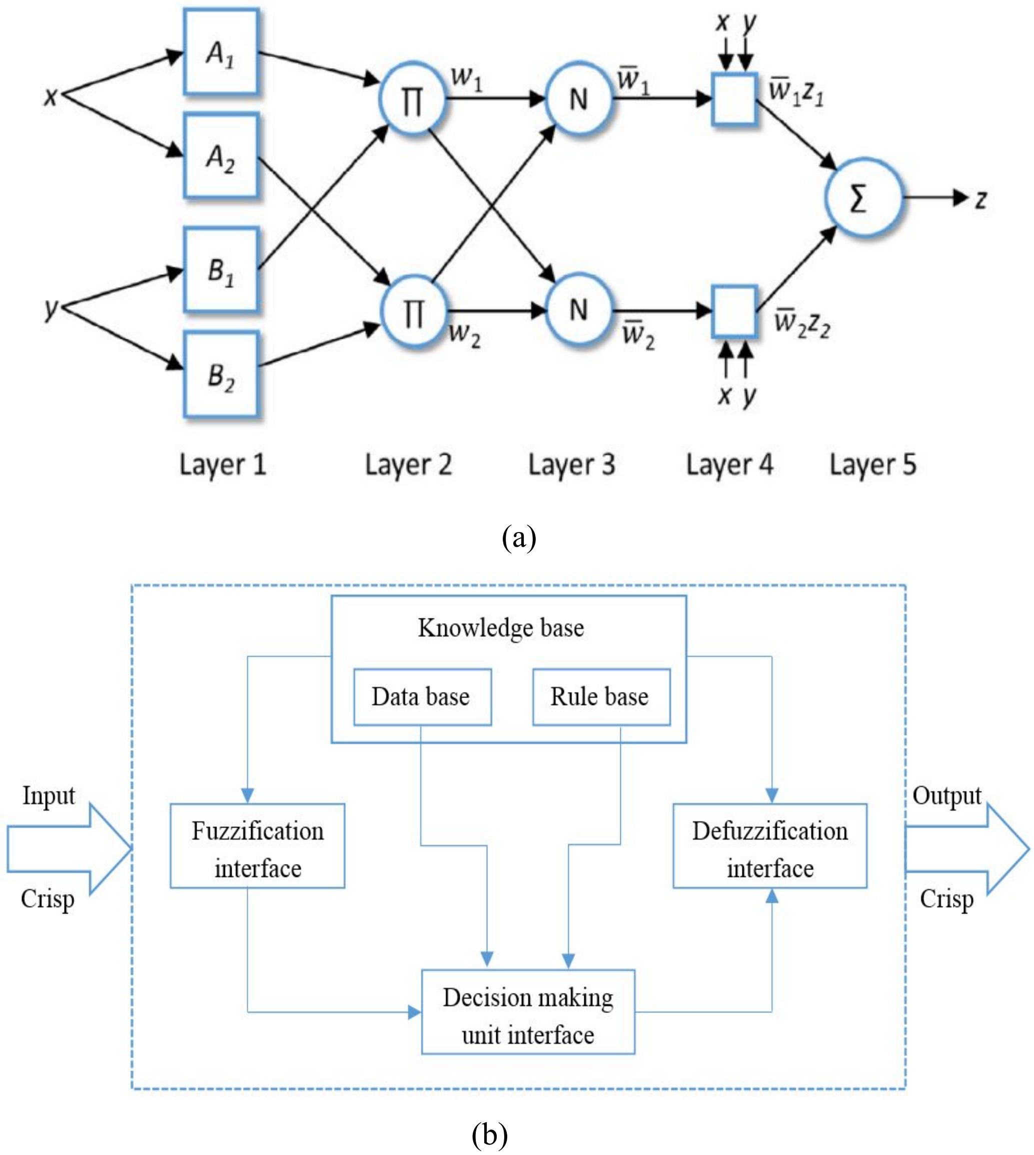


Figure 6. (a) A schematic diagram of ANFIS structure and (b) A schematic diagram of fuzzy based inference system

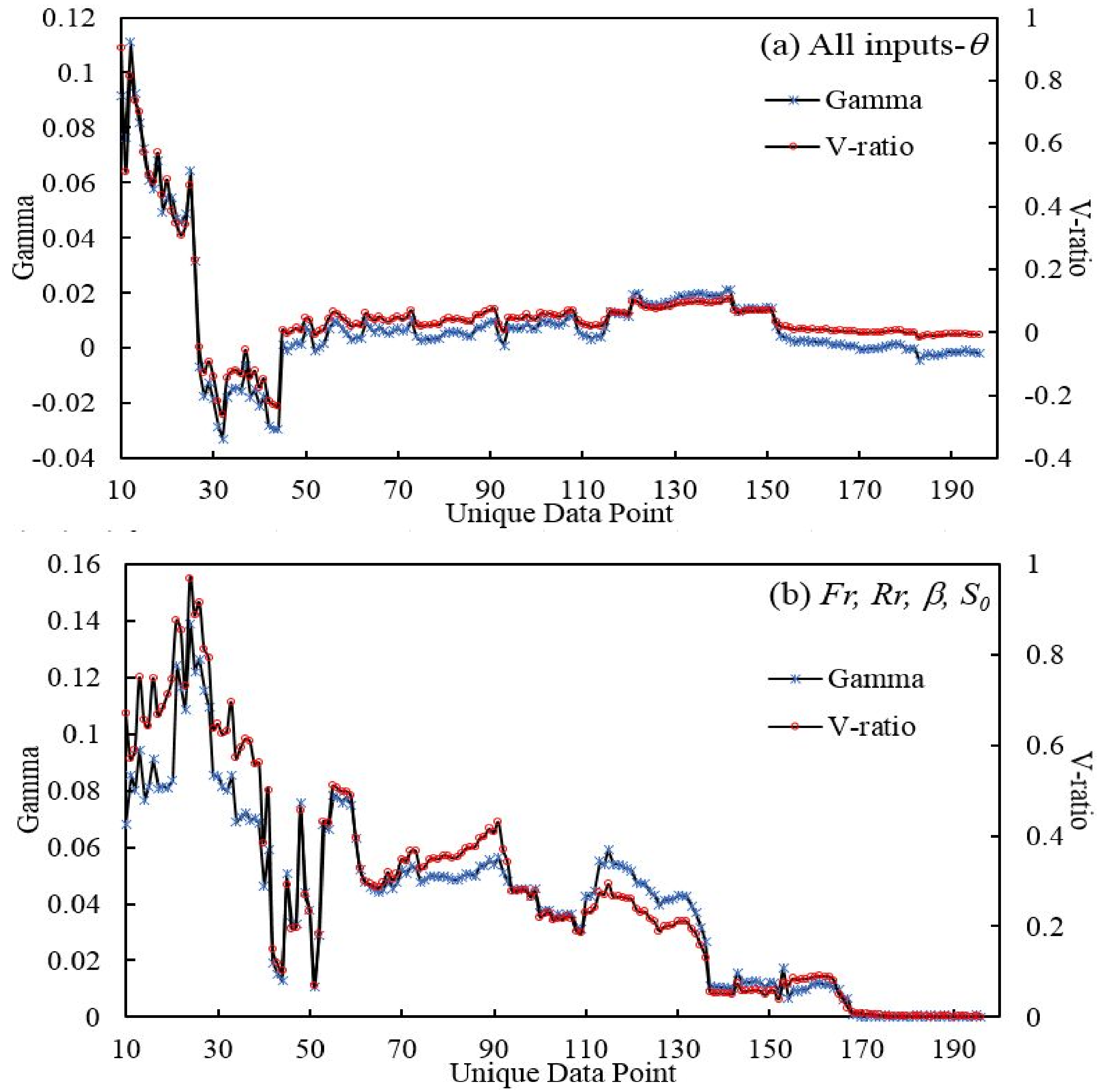


Figure 7. M-test curve: the variation of gamma statistic and V-ratio with unique data points to determining the proper length of training data for mask a) [111111110] and b) [101110000]

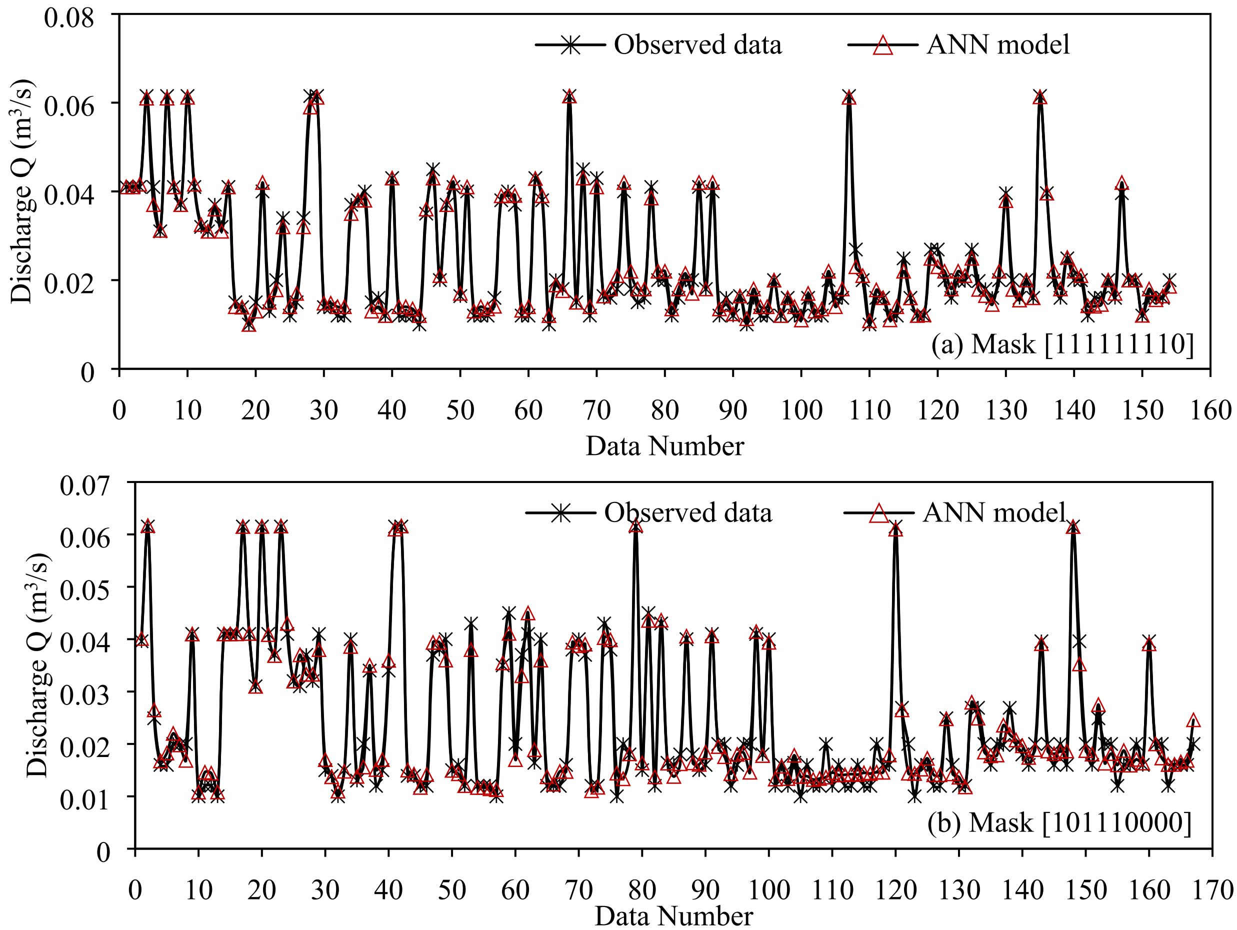


Figure 8. Predicted and observed data for calibration step of ANN model

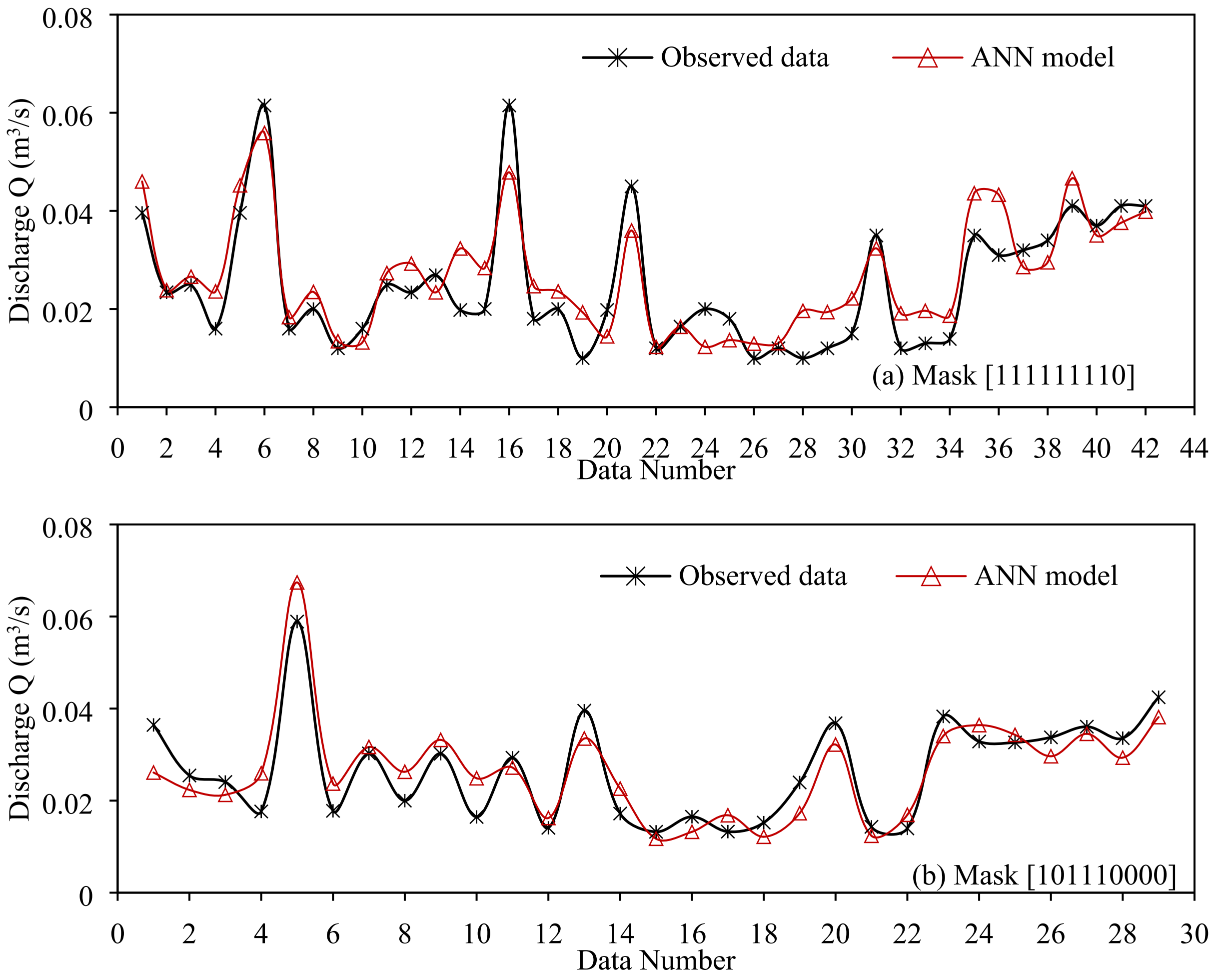


Figure 9. Predicted and observed data for testing step of ANN model

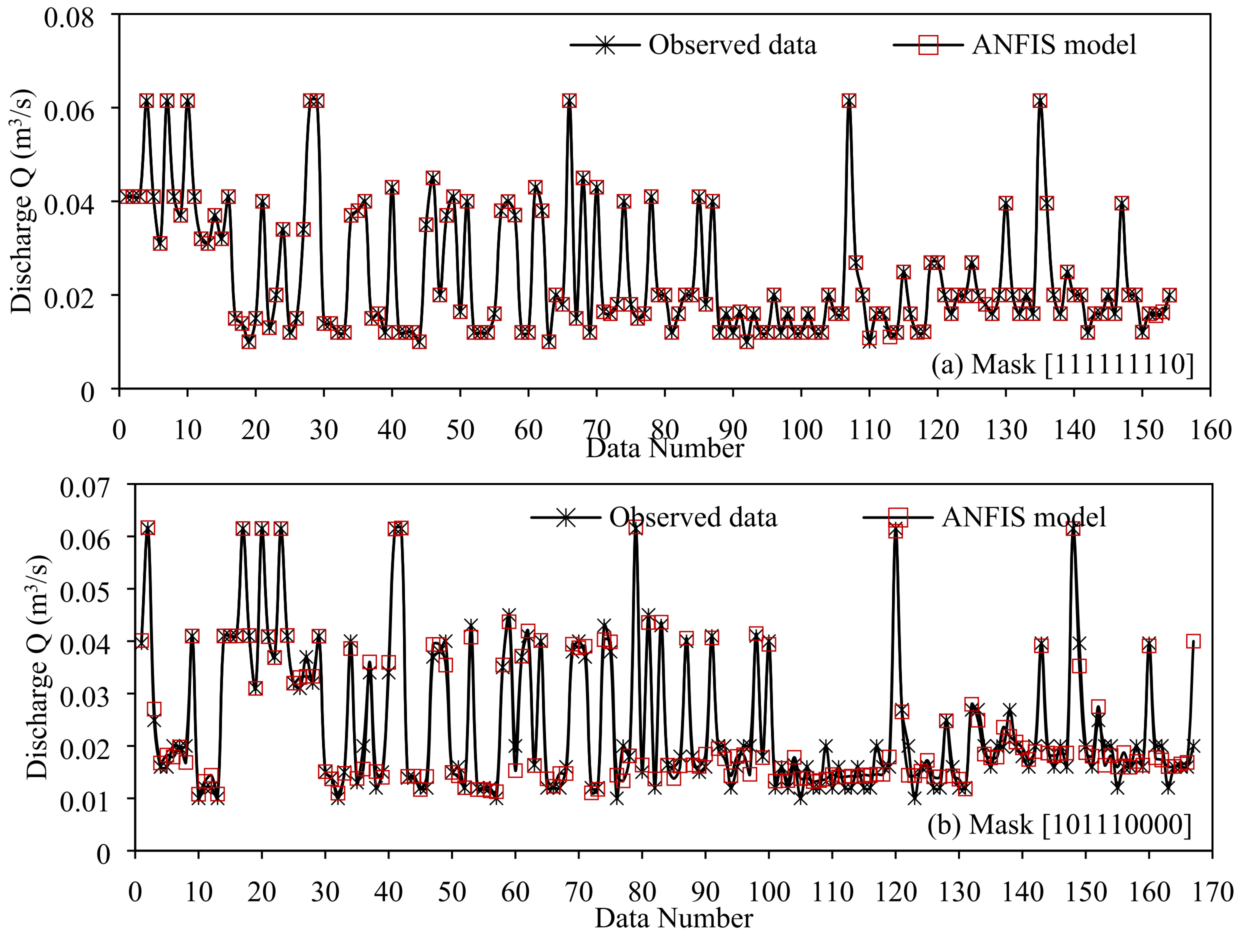


Figure 10. Predicted and observed data for calibration step of ANFIS model

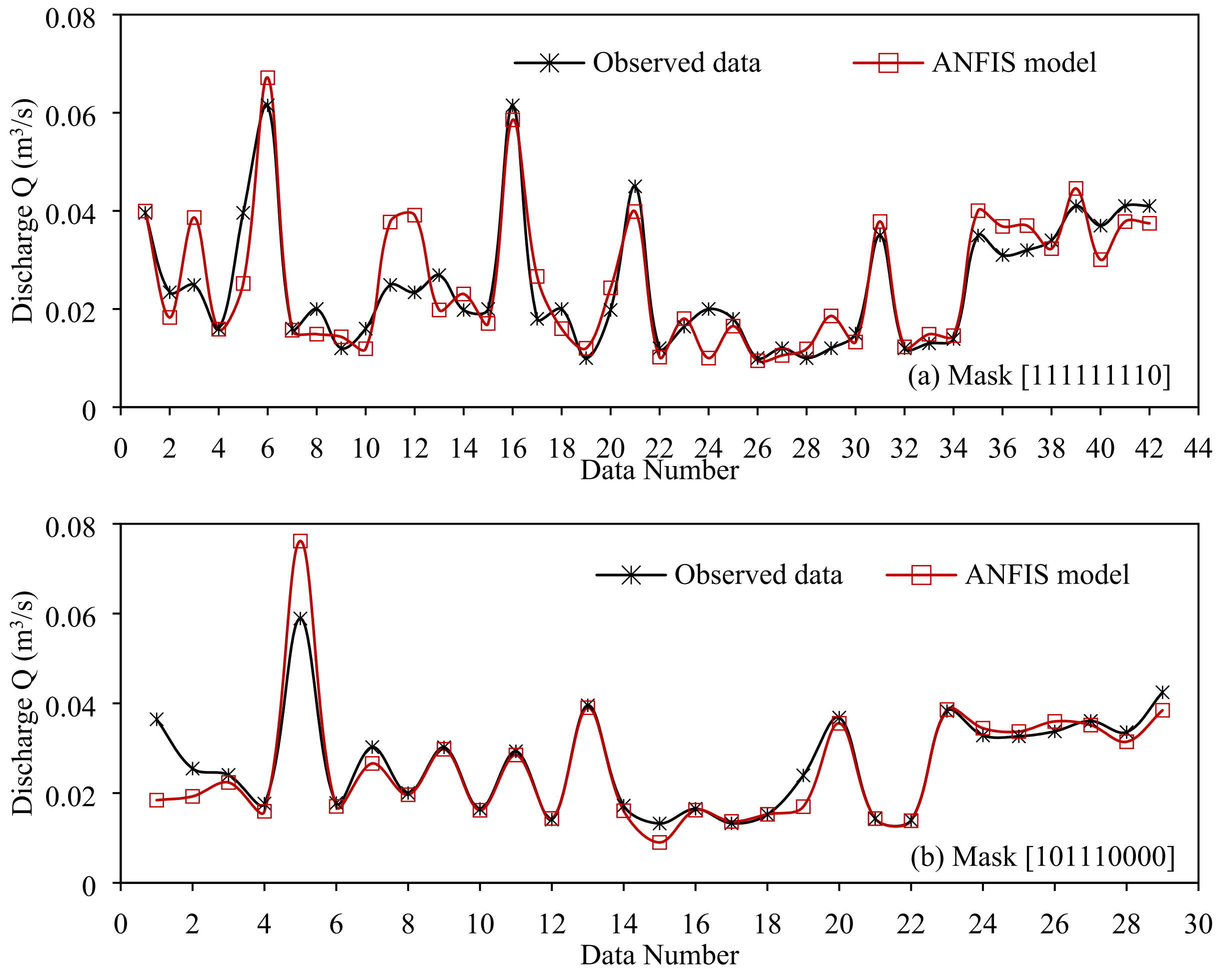


Figure 11. Predicted and observed value for testing step of ANFIS model

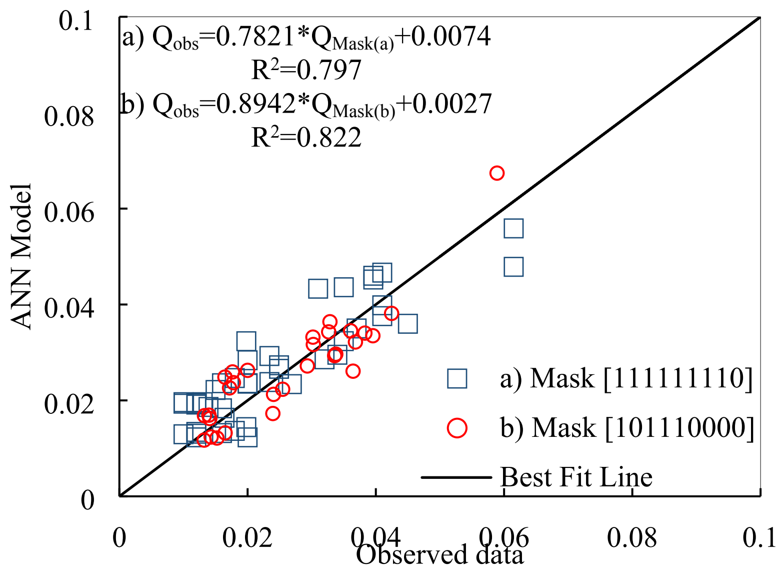


Figure 12. Comparison between the ANN model predicted value and observed value of discharge

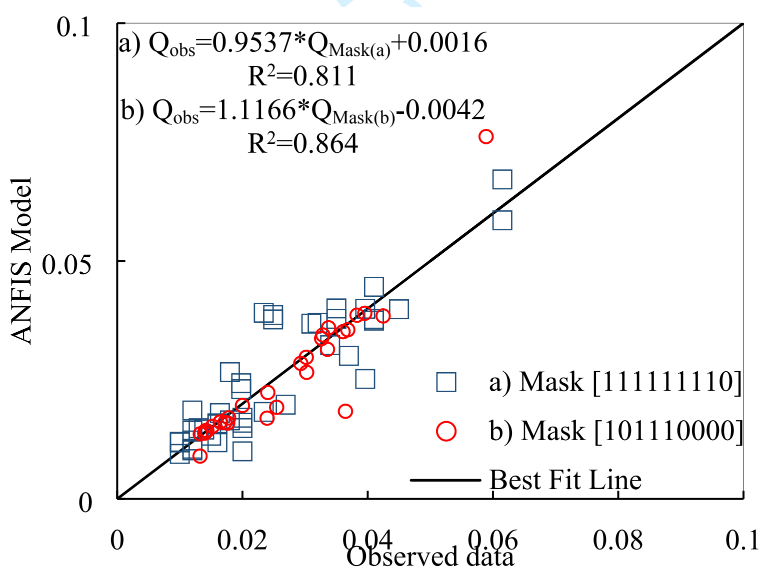


Figure 13. Comparison between the ANFIS model predicted value and observed value of discharge

Table 1. Details of geometric, hydraulic and surface parameters of converging and diverging compound channel collected from published data

| Verified Test Channel | $Q$ in ($m^3$/s) | $n$ | $\beta$ | $S_0$ | $b$ | $h$ | θ | α | δ |
|---|---|---|---|---|---|---|---|---|---|
| 1 | 2 | 3 | 4 | 5 | 6 | 7 | 8 | 9 | 10 |
| B/Cv3.81 | 0.010-0.020 | 0.0107 | 0.213-0.537 | 0.00099 | 0.4 | 0.05 | 3.81 | 1.0-3.0 | 8 |
| B/Cv11.3 | 0.010-0.020 | 0.0107 | 0.18-0.532 | 0.00099 | 0.4 | 0.05 | 11.31 | 1.0-3.0 | 8 |
| B et al./Dv3.81 | 0.012-0.020 | 0.0107 | 0.218-0.514 | 0.00099 | 0.4 | 0.05 | 3.81 | 3.0-1.0 | 8 |
| B et al./Dv5.71 | 0.012-0.020 | 0.0107 | 0.253-0.541 | 0.00099 | 0.4 | 0.05 | 5.71 | 3.0-1.0 | 8 |
| R/Cv1.91 | 0.015-0.040 | 0.0084 | 0.178-0.522 | 0.002003 | 0.398 | 0.05 | 1.91 | 1.0-3.0 | 7.96 |
| R/Cv3.81 | 0.014-0.025 | 0.0091 | 0.151-0.509 | 0.002003 | 0.398 | 0.05 | 3.81 | 1.0-3.0 | 7.96 |
| R/Cv11.31 | 0.013-0.023 | 0.0091 | 0.198-0.505 | 0.002003 | 0.398 | 0.05 | 11.31 | 1.0-3.0 | 7.96 |
| Y et al./Dv3.81 | 0.037-0.0615 | 0.0139 | 0.142-0.363 | 0.00088 | 0.4 | 0.18 | 3.81 | 3.0-1.0 | 2.22 |
| Y et al./Dv5.71 | 0.037-0.0615 | 0.0139 | 0.142-0.352 | 0.00088 | 0.4 | 0.18 | 5.71 | 3.0-1.0 | 2.22 |
| Y et al./Dv11.3 | 0.037-0.0615 | 0.0139 | 0.143-0.359 | 0.00088 | 0.4 | 0.18 | 11.31 | 3.0-1.0 | 2.22 |
| NK /Cv5 | 0.043-0.062 | 0.011 | 0.15-0.30 | 0.0011 | 0.5 | 0.1 | 5 | 1.0-1.8 | 5 |
| NK /Cv9 | 0.042-0.059 | 0.011 | 0.15-0.30 | 0.0011 | 0.5 | 0.1 | 9 | 1.0-1.8 | 5 |
| NK /Cv12.3 | 0.040-0.054 | 0.011 | 0.15-0.30 | 0.0011 | 0.5 | 0.1 | 12.38 | 1.0-1.8 | 5 |

B-Bousmar (2002), B et al.-Bousmar et al. (2006), R- Rezaei (2006), Y et al.- Yonesi et al (2013), NK- Naik and Khatua (2016), Observed discharge in $m^3$/s- $Q$, Manning's roughness coefficient-$n$, Relative depth-$b$, Longitudinal slope-$S_0$, Main channel width in meter- b, Main channel depth in meter -$h$, Converging/Diverging angle in degree - $\theta$, Width ratio- $\alpha$, Aspect ratio-$\delta$

Table 2. Statistical characteristics of the data under consideration

| Statistical characteristics | $F_r$ | $A_r$ | $R_r$ | $\beta$ | $S_0$ | $\delta^*$ | $\alpha$ | $X_r$ | $\theta$ | $Q$ |
|---|---|---|---|---|---|---|---|---|---|---|
| Maximum | 0.84 | 22.59 | 35.09 | 0.54 | 0.002003 | 6.54 | 3.02 | 1.00 | 11.31 | 0.0615 |
| Minimum | 0.31 | 0.93 | 1.70 | 0.11 | 0.000880 | 1.41 | 1.33 | 0.00 | -13.4 | 0.0100 |
| Std. Dev. | 0.09 | 3.73 | 3.15 | 0.12 | 0.000423 | 1.27 | 0.55 | 0.32 | 7.01 | 0.0136 |
| Mean | 0.70 | 4.37 | 3.51 | 0.34 | 0.001226 | 4.40 | 2.10 | 0.42 | -2.17 | 0.0244 |
| Median | 0.71 | 3.00 | 2.80 | 0.33 | 0.000990 | 4.19 | 2.00 | 0.33 | -1.91 | 0.0199 |

Table 3. Error indices result of the analytical approaches

| Methods | $R^2$ | MAE | MAPE | RMSE | E |
|---|---|---|---|---|---|
| SCM | 0.47 | 0.0073 | 43.57 | 0.017 | -3.293 |
| $DCM_{v-e}$ | 0.73 | 0.0079 | 36.93 | 0.011 | -2.990 |
| $DCM_{v-i}$ | 0.74 | 0.0064 | 30.67 | 0.009 | -1.651 |
| $DCM_{h-e}$ | 0.57 | 0.0088 | 41.01 | 0.013 | -4.517 |
| $DCM_{h-i}$ | 0.59 | 0.0073 | 32.50 | 0.010 | -2.032 |
| $DCM_{d-e}$ | 0.72 | 0.0066 | 31.18 | 0.010 | -2.018 |
| $DCM_{d-i}$ | 0.68 | 0.0064 | 26.20 | 0.008 | -0.732 |
| IDCM | 0.51 | 0.0091 | 35.37 | 0.039 | -8.213 |
| EDM | 0.69 | 0.0072 | 32.81 | 0.008 | -0.814 |

Table 4. Determining the best combination for flow ($Q$) in non-prismatic compound channel

| Exp. No. | Combination of Input parameters | Gamma | Std. error | V-ratio | Mask |
|---|---|---|---|---|---|
| 1 | All inputs | -0.009 | 0.006 | -0.036 | 111111111 |
| 2 | All inputs-$f_r$ | -0.006 | 0.005 | -0.027 | 011111111 |
| 3 | All inputs-$\alpha$ | -0.003 | 0.004 | -0.014 | 111111011 |
| 4 | All inputs-$X_r$ | -0.006 | 0.006 | -0.027 | 111111101 |
| **5** | **All inputs-$\theta$** | **-0.001** | **0.007** | **-0.007** | **111111110** |
| 6 | All inputs- $X_r$,$\theta$ | 0.004 | 0.004 | 0.017 | 111111100 |
| 7 | All inputs- $X_r$,$\alpha$ | -0.008 | 0.007 | -0.034 | 111111001 |
| 8 | All inputs- $\theta$, $\delta^*$ | 0.061 | 0.023 | 0.247 | 111110110 |
| 9 | All inputs- $\theta$, $X_r$ | 0.004 | 0.004 | 0.017 | 111111100 |
| 10 | All inputs- $\alpha$ , $X_r$, $\theta$ | 0.008 | 0.003 | 0.034 | 111111000 |
| 11 | All inputs-$A_r$,$R_r$ | -0.011 | 0.006 | -0.045 | 100111111 |
| 12 | All inputs- $A_r$,$R_r$ $\theta$ | 0.003 | 0.007 | 0.014 | 100111110 |
| 13 | $F_r$, $A_r$,$R_r$,$\beta$,$S_0$ | 0.017 | 0.017 | 0.070 | 111110000 |
| 14 | $\alpha$ , $\beta$, $\theta$ , $X_r$, $S_0$, | 0.07 | 0.030 | 0.280 | 000110111 |
| 15 | $\alpha$ , $\beta$, $\delta^*$ , $X_r$, $S_0$ | 0.005 | 0.003 | 0.023 | 000111110 |
| 16 | $F_r$, $A_r$,$R_r$, $S_0$ | 0.054 | 0.020 | 0.216 | 111010000 |
| **17** | **$F_r$, $R_r$,$\beta$, $S_0$** | **0.0002** | **0.010** | **0.001** | **101110000** |
| 18 | $\alpha$ , $\beta$, $S_0$ | 0.097 | 0.053 | 0.388 | 000110100 |
| 19 | $F_r$, $R_r$,$S_0$ | 0.038 | 0.012 | 0.155 | 101010000 |
| 20 | $F_r$, $\beta$,$S_0$ | 0.028 | 0.011 | 0.114 | 100110000 |

Table 5. Different training parameters used for neural network analysis

| Parameter | Value | | Description |
|---|---|---|---|
| | Mask [a] | Mask [b] | |
| Network structures | 8 | 4 | Neuron in the input layer |
| | 10 | 8 | Neuron in the hidden layer |
| | 1 | 1 | Neuron in the output layer |
| net.trainParam.epochs | 1500 | 1500 | Maximum epochs |
| net.trainParam.lr | 0.01 | 0.01 | % learning rate |
| net.trainParam.mu | 0.6 | 0.6 | Momentum parameter |
| net.trainParam.goal | $1 \times 10^{-10}$ | $1\times 10^{-10}$ | Mean square error |
| net.trainParam.grad | 2.58 | 2.72 | Minimum performance gradient |
| net.trainParam. | 1.42 | 1.53 | Maximum performance to increase |
| max_perf_inc<br>net.trainParam.time | inf | inf | Maximum time to train seconds |

Table 6. Details of the best ANFIS model performance

| Subtractive clustering | | Grid partitioning (gaussmf-linear) | |
|---|---|---|---|
| 8 input Parameters | $F_r$, $A_r$, $R_r$, $\beta$, $S_0$, $\delta^*$, $\alpha$, $X_r$ | 4 input Parameters | $F_r$, $R_r$, $\beta$, $S_0$ |
| Rules | 18 | No. of MF | 4444 |
| Range of influence | 0.52 | MF | gaussmf |
| Squash factor | 1.2 | And method | prod |
| Accept ratio | 0.5 | Or method | max |
| Reject ratio | 0.15 | Defuzz method | wtaver |
| Type | Sugeno | Agg method | max |
| $R^2$ (Training) | 0.99 | $R^2$ (Training) | 0.96 |
| $R^2$ (Testing) | 0.82 | $R^2$ (Testing) | 0.86 |
| MAPE (Training) | 1.3% | MAPE (Training) | 8.62% |
| MAPE (Testing) | 16.1% | MAPE (Testing) | 9.42% |
| RMSE (Training) | 0.0001 | RMSE (Training) | 0.0026 |
| RMSE (Testing) | 0.0055 | RMSE (Testing) | 0.0051 |
| MAE (Testing) | 0.003 | MAE (Testing) | 0.0027 |
| E (Testing) | 0.99 | E (Testing) | 0.78 |

Table 7. All nine input variables data of converging and diverging compound channel collected

| Sl no. | | *fr* | *Ar* | *Rr* | $\beta$ | $S_0$ | $\delta^*$ | $\alpha$ | *Xr* | $\theta$ | *Q* |
|---|---|---|---|---|---|---|---|---|---|---|---|
| 1 | R/ Cv3.81 | 0.631 | 2.39 | 3.98 | 0.207 | 0.002003 | 6.31 | 3.02 | 0 | -3.81 | 0.0139 |
| 2 | | 0.635 | 3.09 | 3.91 | 0.214 | 0.002003 | 6.26 | 2.51 | 0.250 | -3.81 | 0.0139 |
| 3 | | 0.621 | 4.85 | 4.17 | 0.203 | 0.002003 | 6.34 | 2.01 | 0.500 | -3.81 | 0.0139 |
| 4 | | 0.607 | 9.76 | 4.46 | 0.202 | 0.002003 | 6.36 | 1.51 | 0.750 | -3.81 | 0.0139 |
| 5 | | 0.710 | 1.65 | 2.79 | 0.301 | 0.002003 | 5.56 | 3.02 | 0.000 | -3.81 | 0.0164 |
| 6 | | 0.719 | 2.07 | 2.69 | 0.320 | 0.002003 | 5.41 | 2.51 | 0.250 | -3.81 | 0.0164 |
| 7 | | 0.702 | 3.23 | 2.89 | 0.306 | 0.002003 | 5.52 | 2.01 | 0.500 | -3.81 | 0.0164 |
| 8 | | 0.668 | 6.90 | 3.36 | 0.285 | 0.002003 | 5.69 | 1.51 | 0.750 | -3.81 | 0.0164 |
| 9 | | 0.773 | 1.24 | 2.17 | 0.400 | 0.002003 | 4.78 | 3.02 | 0.000 | -3.81 | 0.0198 |
| 10 | | 0.771 | 1.62 | 2.18 | 0.409 | 0.002003 | 4.70 | 2.51 | 0.250 | -3.81 | 0.0198 |
| 11 | | 0.756 | 2.45 | 2.31 | 0.404 | 0.002003 | 4.74 | 2.01 | 0.500 | -3.81 | 0.0198 |
| 12 | | 0.719 | 5.03 | 2.69 | 0.390 | 0.002003 | 4.85 | 1.51 | 0.750 | -3.81 | 0.0198 |
| 13 | | 0.824 | 0.98 | 1.79 | 0.504 | 0.002003 | 3.95 | 3.02 | 0.000 | -3.81 | 0.0249 |
| 14 | | 0.816 | 1.30 | 1.84 | 0.509 | 0.002003 | 3.91 | 2.51 | 0.250 | -3.81 | 0.0249 |
| 15 | | 0.795 | 1.97 | 1.99 | 0.503 | 0.002003 | 3.96 | 2.01 | 0.500 | -3.81 | 0.0249 |
| 16 | | 0.746 | 4.02 | 2.41 | 0.488 | 0.002003 | 4.07 | 1.51 | 0.750 | -3.81 | 0.0249 |
| 17 | R\Cv1.91 | 0.602 | 2.77 | 4.59 | 0.179 | 0.002003 | 6.54 | 3.02 | 0.000 | -1.91 | 0.015 |
| 18 | | 0.615 | 2.95 | 4.30 | 0.192 | 0.002003 | 6.43 | 2.76 | 0.250 | -1.91 | 0.015 |
| 19 | | 0.625 | 3.24 | 4.09 | 0.204 | 0.002003 | 6.34 | 2.51 | 0.500 | -1.91 | 0.015 |
| 20 | | 0.642 | 3.55 | 3.78 | 0.224 | 0.002003 | 6.18 | 2.26 | 0.750 | -1.91 | 0.015 |
| 21 | | 0.657 | 4.05 | 3.53 | 0.245 | 0.002003 | 6.01 | 2.01 | 1.000 | -1.91 | 0.015 |
| 22 | | 0.685 | 1.84 | 3.11 | 0.269 | 0.002003 | 5.82 | 3.02 | 0.000 | -1.91 | 0.018 |
| 23 | | 0.705 | 1.91 | 2.85 | 0.297 | 0.002003 | 5.60 | 2.76 | 0.250 | -1.91 | 0.018 |
| 24 | | 0.705 | 2.21 | 2.86 | 0.300 | 0.002003 | 5.57 | 2.51 | 0.500 | -1.91 | 0.018 |
| 25 | | 0.708 | 2.57 | 2.82 | 0.308 | 0.002003 | 5.50 | 2.26 | 0.750 | -1.91 | 0.018 |
| 26 | | 0.712 | 3.07 | 2.77 | 0.322 | 0.002003 | 5.39 | 2.01 | 1.000 | -1.91 | 0.018 |
| 27 | | 0.774 | 1.23 | 2.16 | 0.402 | 0.002003 | 4.76 | 3.02 | 0.000 | -1.91 | 0.0269 |
| 28 | | 0.772 | 1.41 | 2.17 | 0.403 | 0.002003 | 4.75 | 2.76 | 0.250 | -1.91 | 0.0269 |
| 29 | | 0.768 | 1.64 | 2.20 | 0.403 | 0.002003 | 4.75 | 2.51 | 0.500 | -1.91 | 0.0269 |
| 30 | | 0.760 | 2.00 | 2.28 | 0.396 | 0.002003 | 4.81 | 2.26 | 0.750 | -1.91 | 0.0269 |
| 31 | | 0.741 | 2.65 | 2.45 | 0.374 | 0.002003 | 4.98 | 2.01 | 1.000 | -1.91 | 0.0269 |
| 32 | | 0.830 | 0.96 | 1.75 | 0.519 | 0.002003 | 3.83 | 3.02 | 0.000 | -1.91 | 0.0396 |
| 33 | | 0.827 | 1.09 | 1.77 | 0.522 | 0.002003 | 3.80 | 2.76 | 0.250 | -1.91 | 0.0396 |
| 34 | | 0.819 | 1.28 | 1.82 | 0.516 | 0.002003 | 3.85 | 2.51 | 0.500 | -1.91 | 0.0396 |
| 35 | | 0.808 | 1.56 | 1.90 | 0.507 | 0.002003 | 3.92 | 2.26 | 0.750 | -1.91 | 0.0396 |
| 36 | | 0.786 | 2.08 | 2.06 | 0.476 | 0.002003 | 4.17 | 2.01 | 1.000 | -1.91 | 0.0396 |
| 37 | R\ Cv1 | 0.622 | 2.50 | 4.15 | 0.199 | 0.002003 | 6.38 | 3.02 | 0.667 | -11.31 | 0.013 |
| 38 | | 0.619 | 4.92 | 4.22 | 0.202 | 0.002003 | 6.36 | 2.01 | 0.833 | -11.31 | 0.013 |

| | | | | | | | | | | | |
|---|---|---|---|---|---|---|---|---|---|---|---|
| 39 | 1.31 | 0.708 | 1.66 | 2.82 | 0.299 | 0.002003 | 5.58 | 3.02 | 0.667 | -11.31 | 0.015 |
| 40 | | 0.697 | 3.31 | 2.96 | 0.299 | 0.002003 | 5.58 | 2.01 | 0.833 | -11.31 | 0.015 |
| 41 | | 0.774 | 1.23 | 2.16 | 0.402 | 0.002003 | 4.76 | 3.02 | 0.667 | -11.31 | 0.018 |
| 42 | | 0.753 | 2.50 | 2.35 | 0.396 | 0.002003 | 4.81 | 2.01 | 0.833 | -11.31 | 0.018 |
| 43 | | 0.825 | 0.98 | 1.78 | 0.506 | 0.002003 | 3.93 | 3.02 | 0.667 | -11.31 | 0.0234 |
| 44 | | 0.794 | 1.98 | 2.00 | 0.500 | 0.002003 | 3.98 | 2.01 | 0.833 | -11.31 | 0.0234 |
| 45 | B\ Cv3.81 | 0.837 | 0.93 | 1.70 | 0.538 | 0.000990 | 3.69 | 3.00 | 0.000 | -3.81 | 0.02 |
| 46 | | 0.829 | 1.12 | 1.76 | 0.534 | 0.000990 | 3.73 | 2.67 | 0.167 | -3.81 | 0.02 |
| 47 | | 0.817 | 1.42 | 1.83 | 0.529 | 0.000990 | 3.77 | 2.33 | 0.333 | -3.81 | 0.02 |
| 48 | | 0.800 | 1.92 | 1.95 | 0.520 | 0.000990 | 3.84 | 2.00 | 0.500 | -3.81 | 0.02 |
| 49 | | 0.770 | 2.96 | 2.19 | 0.505 | 0.000990 | 3.96 | 1.67 | 0.667 | -3.81 | 0.02 |
| 50 | | 0.709 | 6.13 | 2.81 | 0.487 | 0.000990 | 4.10 | 1.34 | 0.833 | -3.81 | 0.02 |
| 51 | | 0.755 | 1.35 | 2.33 | 0.369 | 0.000990 | 5.05 | 3.00 | 0.000 | -3.81 | 0.012 |
| 52 | | 0.746 | 1.67 | 2.41 | 0.360 | 0.000990 | 5.12 | 2.67 | 0.167 | -3.81 | 0.012 |
| 53 | | 0.734 | 2.15 | 2.53 | 0.348 | 0.000990 | 5.22 | 2.33 | 0.333 | -3.81 | 0.012 |
| 54 | | 0.717 | 3.02 | 2.72 | 0.331 | 0.000990 | 5.35 | 2.00 | 0.500 | -3.81 | 0.012 |
| 55 | | 0.691 | 4.86 | 3.03 | 0.308 | 0.000990 | 5.54 | 1.67 | 0.667 | -3.81 | 0.012 |
| 56 | | 0.646 | 10.72 | 3.70 | 0.278 | 0.000990 | 5.77 | 1.34 | 0.833 | -3.81 | 0.012 |
| 57 | B\ Cv11.31 | 0.692 | 1.80 | 3.02 | 0.278 | 0.000990 | 5.78 | 3.00 | 0.000 | -11.31 | 0.01 |
| 58 | | 0.677 | 2.53 | 3.22 | 0.263 | 0.000990 | 5.89 | 2.50 | 0.083 | -11.31 | 0.01 |
| 59 | | 0.657 | 4.07 | 3.52 | 0.246 | 0.000990 | 6.03 | 2.00 | 0.167 | -11.31 | 0.01 |
| 60 | | 0.610 | 9.71 | 4.40 | 0.205 | 0.000990 | 6.36 | 1.50 | 0.250 | -11.31 | 0.01 |
| 61 | | 0.743 | 1.42 | 2.43 | 0.351 | 0.000990 | 5.19 | 3.00 | 0.000 | -11.31 | 0.01 |
| 62 | | 0.734 | 1.93 | 2.53 | 0.345 | 0.000990 | 5.24 | 2.50 | 0.083 | -11.31 | 0.01 |
| 63 | | 0.721 | 2.96 | 2.67 | 0.338 | 0.000990 | 5.30 | 2.00 | 0.167 | -11.31 | 0.01 |
| 64 | | 0.683 | 6.39 | 3.14 | 0.312 | 0.000990 | 5.50 | 1.50 | 0.250 | -11.31 | 0.01 |
| 65 | | 0.745 | 1.41 | 2.42 | 0.354 | 0.000990 | 5.17 | 3.00 | 0.000 | -11.31 | 0.012 |
| 66 | | 0.734 | 1.93 | 2.53 | 0.345 | 0.000990 | 5.24 | 2.50 | 0.083 | -11.31 | 0.012 |
| 67 | | 0.715 | 3.04 | 2.73 | 0.329 | 0.000990 | 5.37 | 2.00 | 0.167 | -11.31 | 0.012 |
| 68 | | 0.669 | 6.92 | 3.33 | 0.288 | 0.000990 | 5.69 | 1.50 | 0.250 | -11.31 | 0.012 |
| 69 | | 0.832 | 0.95 | 1.74 | 0.524 | 0.000990 | 3.81 | 3.00 | 0.000 | -11.31 | 0.012 |
| 70 | | 0.820 | 1.28 | 1.81 | 0.522 | 0.000990 | 3.82 | 2.50 | 0.083 | -11.31 | 0.012 |
| 71 | | 0.799 | 1.93 | 1.96 | 0.519 | 0.000990 | 3.85 | 2.00 | 0.167 | -11.31 | 0.012 |
| 72 | | 0.749 | 3.90 | 2.38 | 0.511 | 0.000990 | 3.91 | 1.50 | 0.250 | -11.31 | 0.012 |
| 73 | | 0.835 | 0.94 | 1.72 | 0.531 | 0.000990 | 3.75 | 3.00 | 0.000 | -11.31 | 0.016 |
| 74 | | 0.821 | 1.27 | 1.81 | 0.525 | 0.000990 | 3.80 | 2.50 | 0.083 | -11.31 | 0.016 |
| 75 | | 0.800 | 1.92 | 1.95 | 0.521 | 0.000990 | 3.83 | 2.00 | 0.167 | -11.31 | 0.016 |
| 76 | | 0.747 | 3.98 | 2.40 | 0.501 | 0.000990 | 3.99 | 1.50 | 0.250 | -11.31 | 0.016 |
| 77 | | 0.834 | 0.94 | 1.72 | 0.530 | 0.000990 | 3.76 | 3.00 | 0.000 | -11.31 | 0.016 |
| 78 | | 0.821 | 1.27 | 1.81 | 0.525 | 0.000990 | 3.80 | 2.50 | 0.083 | -11.31 | 0.016 |
| 79 | | 0.798 | 1.95 | 1.97 | 0.513 | 0.000990 | 3.90 | 2.00 | 0.167 | -11.31 | 0.016 |

| | | | | | | | | | | |
|---|---|---|---|---|---|---|---|---|---|---|
| 80 | | 0.745 | 4.08 | 2.42 | 0.489 | 0.000990 | 4.09 | 1.50 | 0.250 | -11.31 | 0.016 |
| 81 | B et al\ Dv3.81 | 0.624 | 12.46 | 4.11 | 0.241 | 0.000990 | 6.07 | 1.33 | 0.167 | 3.81 | 0.012 |
| 82 | | 0.648 | 6.15 | 3.68 | 0.244 | 0.000990 | 6.05 | 1.67 | 0.333 | 3.81 | 0.012 |
| 83 | | 0.652 | 4.18 | 3.60 | 0.240 | 0.000990 | 6.08 | 2.00 | 0.500 | 3.81 | 0.012 |
| 84 | | 0.649 | 3.25 | 3.66 | 0.231 | 0.000990 | 6.15 | 2.33 | 0.667 | 3.81 | 0.012 |
| 85 | | 0.636 | 2.80 | 3.89 | 0.214 | 0.000990 | 6.29 | 2.66 | 0.833 | 3.81 | 0.012 |
| 86 | | 0.644 | 2.26 | 3.74 | 0.222 | 0.000990 | 6.23 | 3.00 | 1.000 | 3.81 | 0.012 |
| 87 | | 0.662 | 9.69 | 3.45 | 0.310 | 0.000990 | 5.52 | 1.33 | 0.167 | 3.81 | 0.012 |
| 88 | | 0.699 | 4.67 | 2.93 | 0.322 | 0.000990 | 5.43 | 1.67 | 0.333 | 3.81 | 0.012 |
| 89 | | 0.714 | 3.06 | 2.74 | 0.327 | 0.000990 | 5.38 | 2.00 | 0.500 | 3.81 | 0.012 |
| 90 | | 0.722 | 2.28 | 2.65 | 0.329 | 0.000990 | 5.36 | 2.33 | 0.667 | 3.81 | 0.012 |
| 91 | | 0.722 | 1.86 | 2.66 | 0.323 | 0.000990 | 5.42 | 2.66 | 0.833 | 3.81 | 0.012 |
| 92 | | 0.730 | 1.51 | 2.57 | 0.331 | 0.000990 | 5.35 | 3.00 | 1.000 | 3.81 | 0.012 |
| 93 | | 0.644 | 10.97 | 3.75 | 0.274 | 0.000990 | 5.81 | 1.33 | 0.167 | 3.81 | 0.016 |
| 94 | | 0.704 | 4.54 | 2.87 | 0.331 | 0.000990 | 5.36 | 1.67 | 0.333 | 3.81 | 0.016 |
| 95 | | 0.721 | 2.95 | 2.66 | 0.339 | 0.000990 | 5.29 | 2.00 | 0.500 | 3.81 | 0.016 |
| 96 | | 0.730 | 2.20 | 2.57 | 0.341 | 0.000990 | 5.27 | 2.33 | 0.667 | 3.81 | 0.016 |
| 97 | | 0.732 | 1.78 | 2.55 | 0.338 | 0.000990 | 5.30 | 2.66 | 0.833 | 3.81 | 0.016 |
| 98 | | 0.740 | 1.45 | 2.47 | 0.346 | 0.000990 | 5.24 | 3.00 | 1.000 | 3.81 | 0.016 |
| 99 | | 0.620 | 12.80 | 4.20 | 0.235 | 0.000990 | 6.12 | 1.33 | 0.167 | 3.81 | 0.02 |
| 100 | | 0.683 | 5.10 | 3.14 | 0.295 | 0.000990 | 5.64 | 1.67 | 0.333 | 3.81 | 0.02 |
| 101 | | 0.710 | 3.13 | 2.80 | 0.320 | 0.000990 | 5.44 | 2.00 | 0.500 | 3.81 | 0.02 |
| 102 | | 0.725 | 2.25 | 2.62 | 0.334 | 0.000990 | 5.33 | 2.33 | 0.667 | 3.81 | 0.02 |
| 103 | | 0.742 | 1.70 | 2.45 | 0.354 | 0.000990 | 5.17 | 2.66 | 0.833 | 3.81 | 0.02 |
| 104 | | 0.738 | 1.46 | 2.49 | 0.342 | 0.000990 | 5.26 | 3.00 | 1.000 | 3.81 | 0.02 |
| 105 | | 0.709 | 6.09 | 2.81 | 0.493 | 0.000990 | 4.06 | 1.33 | 0.167 | 3.81 | 0.016 |
| 106 | | 0.770 | 2.97 | 2.19 | 0.506 | 0.000990 | 3.95 | 1.67 | 0.333 | 3.81 | 0.016 |
| 107 | | 0.798 | 1.95 | 1.97 | 0.514 | 0.000990 | 3.89 | 2.00 | 0.500 | 3.81 | 0.016 |
| 108 | | 0.812 | 1.46 | 1.87 | 0.513 | 0.000990 | 3.89 | 2.33 | 0.667 | 3.81 | 0.016 |
| 109 | | 0.824 | 1.16 | 1.79 | 0.519 | 0.000990 | 3.85 | 2.66 | 0.833 | 3.81 | 0.016 |
| 110 | | 0.832 | 0.95 | 1.73 | 0.525 | 0.000990 | 3.80 | 3.00 | 1.000 | 3.81 | 0.016 |
| 111 | | 0.709 | 6.01 | 2.80 | 0.499 | 0.000990 | 4.00 | 1.33 | 0.167 | 3.81 | 0.02 |
| 112 | | 0.769 | 2.99 | 2.20 | 0.503 | 0.000990 | 3.98 | 1.67 | 0.333 | 3.81 | 0.02 |
| 113 | | 0.797 | 1.96 | 1.97 | 0.512 | 0.000990 | 3.90 | 2.00 | 0.500 | 3.81 | 0.02 |
| 114 | | 0.812 | 1.47 | 1.87 | 0.512 | 0.000990 | 3.91 | 2.33 | 0.667 | 3.81 | 0.02 |
| 115 | | 0.822 | 1.16 | 1.80 | 0.516 | 0.000990 | 3.87 | 2.66 | 0.833 | 3.81 | 0.02 |
| 116 | | 0.828 | 0.97 | 1.76 | 0.515 | 0.000990 | 3.88 | 3.00 | 1.000 | 3.81 | 0.02 |
| 117 | B et al./ Dv5.71 | 0.638 | 11.38 | 3.85 | 0.264 | 0.000990 | 5.89 | 1.33 | 0.250 | 5.71 | 0.012 |
| 118 | | 0.670 | 5.47 | 3.33 | 0.275 | 0.000990 | 5.80 | 1.67 | 0.500 | 5.71 | 0.012 |
| 119 | | 0.682 | 3.60 | 3.16 | 0.278 | 0.000990 | 5.78 | 2.00 | 0.750 | 5.71 | 0.012 |
| 120 | | 0.681 | 2.78 | 3.17 | 0.270 | 0.000990 | 5.84 | 2.33 | 1.000 | 5.71 | 0.012 |

| | | | | | | | | | | | |
|---|---|---|---|---|---|---|---|---|---|---|---|
| 121 | | 0.670 | 9.12 | 3.33 | 0.329 | 0.000990 | 5.37 | 1.33 | 0.250 | 5.71 | 0.012 |
| 122 | | 0.709 | 4.40 | 2.80 | 0.341 | 0.000990 | 5.27 | 1.67 | 0.500 | 5.71 | 0.012 |
| 123 | | 0.726 | 2.89 | 2.61 | 0.347 | 0.000990 | 5.22 | 2.00 | 0.750 | 5.71 | 0.012 |
| 124 | | 0.731 | 2.18 | 2.56 | 0.344 | 0.000990 | 5.25 | 2.33 | 1.000 | 5.71 | 0.012 |
| 125 | | 0.675 | 8.79 | 3.25 | 0.342 | 0.000990 | 5.27 | 1.33 | 0.250 | 5.71 | 0.016 |
| 126 | | 0.716 | 4.25 | 2.73 | 0.353 | 0.000990 | 5.17 | 1.67 | 0.500 | 5.71 | 0.016 |
| 127 | | 0.740 | 2.69 | 2.47 | 0.373 | 0.000990 | 5.02 | 2.00 | 0.750 | 5.71 | 0.016 |
| 128 | | 0.743 | 2.06 | 2.43 | 0.364 | 0.000990 | 5.09 | 2.33 | 1.000 | 5.71 | 0.016 |
| 129 | | 0.660 | 9.80 | 3.48 | 0.307 | 0.000990 | 5.55 | 1.33 | 0.250 | 5.71 | 0.02 |
| 130 | | 0.711 | 4.36 | 2.78 | 0.344 | 0.000990 | 5.25 | 1.67 | 0.500 | 5.71 | 0.02 |
| 131 | | 0.740 | 2.69 | 2.47 | 0.373 | 0.000990 | 5.02 | 2.00 | 0.750 | 5.71 | 0.02 |
| 132 | | 0.754 | 1.96 | 2.33 | 0.383 | 0.000990 | 4.93 | 2.33 | 1.000 | 5.71 | 0.02 |
| 133 | | 0.710 | 5.79 | 2.79 | 0.519 | 0.000990 | 3.85 | 1.33 | 0.250 | 5.71 | 0.016 |
| 134 | | 0.775 | 2.84 | 2.15 | 0.529 | 0.000990 | 3.77 | 1.67 | 0.500 | 5.71 | 0.016 |
| 135 | | 0.804 | 1.86 | 1.92 | 0.538 | 0.000990 | 3.70 | 2.00 | 0.750 | 5.71 | 0.016 |
| 136 | | 0.821 | 1.39 | 1.81 | 0.539 | 0.000990 | 3.69 | 2.33 | 1.000 | 5.71 | 0.016 |
| 137 | | 0.710 | 5.76 | 2.79 | 0.522 | 0.000990 | 3.83 | 1.33 | 0.250 | 5.71 | 0.02 |
| 138 | | 0.776 | 2.79 | 2.14 | 0.537 | 0.000990 | 3.70 | 1.67 | 0.500 | 5.71 | 0.02 |
| 139 | | 0.804 | 1.86 | 1.92 | 0.537 | 0.000990 | 3.70 | 2.00 | 0.750 | 5.71 | 0.02 |
| 140 | | 0.820 | 1.40 | 1.81 | 0.537 | 0.000990 | 3.70 | 2.33 | 1.000 | 5.71 | 0.02 |
| 141./ | Y et al /Dv3.81 | 0.305 | 20.60 | 35.09 | 0.146 | 0.000880 | 1.90 | 1.33 | 0.167 | 3.81 | 0.041 |
| 142 | | 0.384 | 10.37 | 17.69 | 0.145 | 0.000880 | 1.90 | 1.67 | 0.333 | 3.81 | 0.041 |
| 143 | | 0.446 | 6.65 | 11.24 | 0.151 | 0.000880 | 1.89 | 2.00 | 0.500 | 3.81 | 0.041 |
| 144 | | 0.500 | 4.76 | 7.98 | 0.158 | 0.000880 | 1.87 | 2.33 | 0.667 | 3.81 | 0.041 |
| 145 | | 0.552 | 3.59 | 5.94 | 0.167 | 0.000880 | 1.85 | 2.66 | 0.833 | 3.81 | 0.041 |
| 146 | | 0.594 | 2.91 | 4.78 | 0.172 | 0.000880 | 1.84 | 3.00 | 1.000 | 3.81 | 0.041 |
| 147 | | 0.432 | 8.83 | 12.44 | 0.340 | 0.000880 | 1.47 | 1.33 | 0.167 | 3.81 | 0.0615 |
| 148 | | 0.548 | 4.34 | 6.09 | 0.346 | 0.000880 | 1.45 | 1.67 | 0.333 | 3.81 | 0.0615 |
| 149 | | 0.631 | 2.85 | 3.99 | 0.351 | 0.000880 | 1.44 | 2.00 | 0.500 | 3.81 | 0.0615 |
| 150 | | 0.696 | 2.13 | 2.97 | 0.353 | 0.000880 | 1.44 | 2.33 | 0.667 | 3.81 | 0.0615 |
| 151 | | 0.754 | 1.67 | 2.33 | 0.359 | 0.000880 | 1.42 | 2.66 | 0.833 | 3.81 | 0.0615 |
| 152 | | 0.806 | 1.37 | 1.91 | 0.364 | 0.000880 | 1.41 | 3.00 | 1.000 | 3.81 | 0.0615 |
| 153 | Y et al/ Dv 11.31 | 0.372 | 11.41 | 19.43 | 0.146 | 0.000880 | 1.90 | 1.60 | 0.100 | 11.31 | 0.041 |
| 154 | | 0.450 | 6.51 | 10.97 | 0.154 | 0.000880 | 1.88 | 2.00 | 0.167 | 11.31 | 0.041 |
| 155 | | 0.534 | 3.92 | 6.56 | 0.159 | 0.000880 | 1.87 | 2.60 | 0.267 | 11.31 | 0.041 |
| 156 | | 0.576 | 3.14 | 5.25 | 0.159 | 0.000880 | 1.87 | 3.00 | 0.333 | 11.31 | 0.041 |
| 157 | | 0.526 | 4.89 | 6.87 | 0.341 | 0.000880 | 1.46 | 1.60 | 0.100 | 11.31 | 0.0615 |
| 158 | | 0.630 | 2.85 | 4.00 | 0.351 | 0.000880 | 1.44 | 2.00 | 0.167 | 11.31 | 0.0615 |
| 159 | | 0.741 | 1.76 | 2.46 | 0.355 | 0.000880 | 1.43 | 2.60 | 0.267 | 11.31 | 0.0615 |
| 160 | | 0.801 | 1.39 | 1.94 | 0.359 | 0.000880 | 1.42 | 3.00 | 0.333 | 11.31 | 0.0615 |
| 161 | N | 0.584 | 8.02 | 5.01 | 0.156 | 0.001100 | 4.22 | 1.80 | 0.000 | -5 | 0.037 |

| | | | | | | | | | | | |
|---|---|---|---|---|---|---|---|---|---|---|---|
| 162 | K/ Cv 5 | 0.547 | 10.37 | 6.09 | 0.126 | 0.001100 | 4.37 | 1.77 | 0.044 | -5 | 0.037 |
| 163 | | 0.527 | 21.08 | 6.85 | 0.118 | 0.001100 | 4.41 | 1.40 | 0.500 | -5 | 0.037 |
| 164 | | 0.678 | 4.76 | 3.21 | 0.262 | 0.001100 | 3.69 | 1.80 | 0.000 | -5 | 0.04 |
| 165 | | 0.640 | 6.10 | 3.81 | 0.214 | 0.001100 | 3.93 | 1.77 | 0.044 | -5 | 0.04 |
| 166 | | 0.617 | 11.72 | 4.26 | 0.213 | 0.001100 | 3.94 | 1.40 | 0.500 | -5 | 0.04 |
| 167 | | 0.701 | 4.18 | 2.90 | 0.299 | 0.001100 | 3.51 | 1.80 | 0.000 | -5 | 0.043 |
| 168 | | 0.682 | 4.83 | 3.15 | 0.271 | 0.001100 | 3.65 | 1.77 | 0.044 | -5 | 0.043 |
| 169 | | 0.646 | 9.60 | 3.71 | 0.260 | 0.001100 | 3.70 | 1.40 | 0.500 | -5 | 0.043 |
| 170 | | 0.716 | 3.85 | 2.73 | 0.325 | 0.001100 | 3.37 | 1.80 | 0.000 | -5 | 0.045 |
| 171 | | 0.697 | 4.43 | 2.95 | 0.295 | 0.001100 | 3.52 | 1.77 | 0.044 | -5 | 0.045 |
| 172 | | 0.660 | 8.67 | 3.48 | 0.288 | 0.001100 | 3.56 | 1.40 | 0.500 | -5 | 0.045 |
| 173 | NK/ Cv 9 | 0.593 | 7.65 | 4.80 | 0.163 | 0.001100 | 4.18 | 1.80 | 0.000 | -9 | 0.032 |
| 174 | | 0.588 | 8.48 | 4.92 | 0.160 | 0.001100 | 4.20 | 1.74 | 0.079 | -9 | 0.032 |
| 175 | | 0.573 | 15.59 | 5.31 | 0.160 | 0.001100 | 4.20 | 1.40 | 0.500 | -9 | 0.032 |
| 176 | | 0.659 | 5.30 | 3.50 | 0.236 | 0.001100 | 3.82 | 1.80 | 0.000 | -9 | 0.035 |
| 177 | | 0.655 | 5.79 | 3.55 | 0.234 | 0.001100 | 3.83 | 1.74 | 0.079 | -9 | 0.035 |
| 178 | | 0.614 | 11.95 | 4.32 | 0.209 | 0.001100 | 3.96 | 1.40 | 0.500 | -9 | 0.035 |
| 179 | | 0.683 | 4.65 | 3.15 | 0.269 | 0.001100 | 3.66 | 1.80 | 0.000 | -9 | 0.038 |
| 180 | | 0.677 | 5.12 | 3.22 | 0.265 | 0.001100 | 3.67 | 1.74 | 0.079 | -9 | 0.038 |
| 181 | | 0.639 | 10.11 | 3.84 | 0.247 | 0.001100 | 3.77 | 1.40 | 0.500 | -9 | 0.038 |
| 182 | | 0.712 | 3.94 | 2.77 | 0.317 | 0.001100 | 3.41 | 1.80 | 0.000 | -9 | 0.041 |
| 183 | | 0.709 | 4.25 | 2.81 | 0.319 | 0.001100 | 3.40 | 1.74 | 0.079 | -9 | 0.041 |
| 184 | | 0.667 | 8.18 | 3.37 | 0.305 | 0.001100 | 3.48 | 1.40 | 0.500 | -9 | 0.041 |
| 185 | NK/ Cv 13.38 | 0.601 | 7.32 | 4.62 | 0.171 | 0.001100 | 4.15 | 1.80 | 0.000 | -13.38 | 0.031 |
| 186 | | 0.575 | 9.52 | 5.27 | 0.149 | 0.001100 | 4.25 | 1.70 | 0.119 | -13.38 | 0.031 |
| 187 | | 0.516 | 22.59 | 7.26 | 0.111 | 0.001100 | 4.45 | 1.40 | 0.595 | -13.38 | 0.031 |
| 188 | | 0.630 | 6.23 | 4.01 | 0.201 | 0.001100 | 4.00 | 1.80 | 0.000 | -13.38 | 0.034 |
| 189 | | 0.622 | 7.26 | 4.16 | 0.195 | 0.001100 | 4.02 | 1.70 | 0.119 | -13.38 | 0.034 |
| 190 | | 0.591 | 13.87 | 4.84 | 0.180 | 0.001100 | 4.10 | 1.40 | 0.595 | -13.38 | 0.034 |
| 191 | | 0.679 | 4.73 | 3.19 | 0.264 | 0.001100 | 3.68 | 1.80 | 0.000 | -13.38 | 0.037 |
| 192 | | 0.665 | 5.68 | 3.40 | 0.250 | 0.001100 | 3.75 | 1.70 | 0.119 | -13.38 | 0.037 |
| 193 | | 0.638 | 10.12 | 3.84 | 0.247 | 0.001100 | 3.77 | 1.40 | 0.595 | -13.38 | 0.037 |
| 194 | | 0.715 | 3.86 | 2.73 | 0.324 | 0.001100 | 3.38 | 1.80 | 0.000 | -13.38 | 0.04 |
| 195 | | 0.707 | 4.45 | 2.83 | 0.319 | 0.001100 | 3.40 | 1.70 | 0.119 | -13.38 | 0.04 |
| 196 | | 0.669 | 8.04 | 3.34 | 0.311 | 0.001100 | 3.45 | 1.40 | 0.595 | -13.38 | 0.04 |

Canadian Journal of Civil Engineering

Appendix: All nine input variables data of converging and diverging compound channel collected

| Sl no. | | *fr* | *Ar* | *Rr* | *β* | $S_0$ | *δ** | *α* | *Xr* | *θ* | *Q* |
|---|---|---|---|---|---|---|---|---|---|---|---|
| 1 | R/ Cv3.81 | 0.631 | 2.39 | 3.98 | 0.207 | 0.002003 | 6.31 | 3.02 | 0 | -3.81 | 0.0139 |
| 2 | | 0.635 | 3.09 | 3.91 | 0.214 | 0.002003 | 6.26 | 2.51 | 0.250 | -3.81 | 0.0139 |
| 3 | | 0.621 | 4.85 | 4.17 | 0.203 | 0.002003 | 6.34 | 2.01 | 0.500 | -3.81 | 0.0139 |
| 4 | | 0.607 | 9.76 | 4.46 | 0.202 | 0.002003 | 6.36 | 1.51 | 0.750 | -3.81 | 0.0139 |
| 5 | | 0.710 | 1.65 | 2.79 | 0.301 | 0.002003 | 5.56 | 3.02 | 0.000 | -3.81 | 0.0164 |
| 6 | | 0.719 | 2.07 | 2.69 | 0.320 | 0.002003 | 5.41 | 2.51 | 0.250 | -3.81 | 0.0164 |
| 7 | | 0.702 | 3.23 | 2.89 | 0.306 | 0.002003 | 5.52 | 2.01 | 0.500 | -3.81 | 0.0164 |
| 8 | | 0.668 | 6.90 | 3.36 | 0.285 | 0.002003 | 5.69 | 1.51 | 0.750 | -3.81 | 0.0164 |
| 9 | | 0.773 | 1.24 | 2.17 | 0.400 | 0.002003 | 4.78 | 3.02 | 0.000 | -3.81 | 0.0198 |
| 10 | | 0.771 | 1.62 | 2.18 | 0.409 | 0.002003 | 4.70 | 2.51 | 0.250 | -3.81 | 0.0198 |
| 11 | | 0.756 | 2.45 | 2.31 | 0.404 | 0.002003 | 4.74 | 2.01 | 0.500 | -3.81 | 0.0198 |
| 12 | | 0.719 | 5.03 | 2.69 | 0.390 | 0.002003 | 4.85 | 1.51 | 0.750 | -3.81 | 0.0198 |
| 13 | | 0.824 | 0.98 | 1.79 | 0.504 | 0.002003 | 3.95 | 3.02 | 0.000 | -3.81 | 0.0249 |
| 14 | | 0.816 | 1.30 | 1.84 | 0.509 | 0.002003 | 3.91 | 2.51 | 0.250 | -3.81 | 0.0249 |
| 15 | | 0.795 | 1.97 | 1.99 | 0.503 | 0.002003 | 3.96 | 2.01 | 0.500 | -3.81 | 0.0249 |
| 16 | | 0.746 | 4.02 | 2.41 | 0.488 | 0.002003 | 4.07 | 1.51 | 0.750 | -3.81 | 0.0249 |
| 17 | R\Cv1.91 | 0.602 | 2.77 | 4.59 | 0.179 | 0.002003 | 6.54 | 3.02 | 0.000 | -1.91 | 0.015 |
| 18 | | 0.615 | 2.95 | 4.30 | 0.192 | 0.002003 | 6.43 | 2.76 | 0.250 | -1.91 | 0.015 |
| 19 | | 0.625 | 3.24 | 4.09 | 0.204 | 0.002003 | 6.34 | 2.51 | 0.500 | -1.91 | 0.015 |
| 20 | | 0.642 | 3.55 | 3.78 | 0.224 | 0.002003 | 6.18 | 2.26 | 0.750 | -1.91 | 0.015 |
| 21 | | 0.657 | 4.05 | 3.53 | 0.245 | 0.002003 | 6.01 | 2.01 | 1.000 | -1.91 | 0.015 |
| 22 | | 0.685 | 1.84 | 3.11 | 0.269 | 0.002003 | 5.82 | 3.02 | 0.000 | -1.91 | 0.018 |
| 23 | | 0.705 | 1.91 | 2.85 | 0.297 | 0.002003 | 5.60 | 2.76 | 0.250 | -1.91 | 0.018 |
| 24 | | 0.705 | 2.21 | 2.86 | 0.300 | 0.002003 | 5.57 | 2.51 | 0.500 | -1.91 | 0.018 |
| 25 | | 0.708 | 2.57 | 2.82 | 0.308 | 0.002003 | 5.50 | 2.26 | 0.750 | -1.91 | 0.018 |
| 26 | | 0.712 | 3.07 | 2.77 | 0.322 | 0.002003 | 5.39 | 2.01 | 1.000 | -1.91 | 0.018 |
| 27 | | 0.774 | 1.23 | 2.16 | 0.402 | 0.002003 | 4.76 | 3.02 | 0.000 | -1.91 | 0.0269 |
| 28 | | 0.772 | 1.41 | 2.17 | 0.403 | 0.002003 | 4.75 | 2.76 | 0.250 | -1.91 | 0.0269 |
| 29 | | 0.768 | 1.64 | 2.20 | 0.403 | 0.002003 | 4.75 | 2.51 | 0.500 | -1.91 | 0.0269 |
| 30 | | 0.760 | 2.00 | 2.28 | 0.396 | 0.002003 | 4.81 | 2.26 | 0.750 | -1.91 | 0.0269 |
| 31 | | 0.741 | 2.65 | 2.45 | 0.374 | 0.002003 | 4.98 | 2.01 | 1.000 | -1.91 | 0.0269 |
| 32 | | 0.830 | 0.96 | 1.75 | 0.519 | 0.002003 | 3.83 | 3.02 | 0.000 | -1.91 | 0.0396 |
| 33 | | 0.827 | 1.09 | 1.77 | 0.522 | 0.002003 | 3.80 | 2.76 | 0.250 | -1.91 | 0.0396 |
| 34 | | 0.819 | 1.28 | 1.82 | 0.516 | 0.002003 | 3.85 | 2.51 | 0.500 | -1.91 | 0.0396 |
| 35 | | 0.808 | 1.56 | 1.90 | 0.507 | 0.002003 | 3.92 | 2.26 | 0.750 | -1.91 | 0.0396 |
| 36 | | 0.786 | 2.08 | 2.06 | 0.476 | 0.002003 | 4.17 | 2.01 | 1.000 | -1.91 | 0.0396 |
| 37 | R\ Cv11.31 | 0.622 | 2.50 | 4.15 | 0.199 | 0.002003 | 6.38 | 3.02 | 0.667 | -11.31 | 0.013 |
| 38 | | 0.619 | 4.92 | 4.22 | 0.202 | 0.002003 | 6.36 | 2.01 | 0.833 | -11.31 | 0.013 |
| 39 | | 0.708 | 1.66 | 2.82 | 0.299 | 0.002003 | 5.58 | 3.02 | 0.667 | -11.31 | 0.015 |

| | | | | | | | | | | | |
|---|---|---|---|---|---|---|---|---|---|---|---|
| 40 | | 0.697 | 3.31 | 2.96 | 0.299 | 0.002003 | 5.58 | 2.01 | 0.833 | -11.31 | 0.015 |
| 41 | | 0.774 | 1.23 | 2.16 | 0.402 | 0.002003 | 4.76 | 3.02 | 0.667 | -11.31 | 0.018 |
| 42 | | 0.753 | 2.50 | 2.35 | 0.396 | 0.002003 | 4.81 | 2.01 | 0.833 | -11.31 | 0.018 |
| 43 | | 0.825 | 0.98 | 1.78 | 0.506 | 0.002003 | 3.93 | 3.02 | 0.667 | -11.31 | 0.0234 |
| 44 | | 0.794 | 1.98 | 2.00 | 0.500 | 0.002003 | 3.98 | 2.01 | 0.833 | -11.31 | 0.0234 |
| 45 | B\ Cv3.81 | 0.837 | 0.93 | 1.70 | 0.538 | 0.000990 | 3.69 | 3.00 | 0.000 | -3.81 | 0.02 |
| 46 | | 0.829 | 1.12 | 1.76 | 0.534 | 0.000990 | 3.73 | 2.67 | 0.167 | -3.81 | 0.02 |
| 47 | | 0.817 | 1.42 | 1.83 | 0.529 | 0.000990 | 3.77 | 2.33 | 0.333 | -3.81 | 0.02 |
| 48 | | 0.800 | 1.92 | 1.95 | 0.520 | 0.000990 | 3.84 | 2.00 | 0.500 | -3.81 | 0.02 |
| 49 | | 0.770 | 2.96 | 2.19 | 0.505 | 0.000990 | 3.96 | 1.67 | 0.667 | -3.81 | 0.02 |
| 50 | | 0.709 | 6.13 | 2.81 | 0.487 | 0.000990 | 4.10 | 1.34 | 0.833 | -3.81 | 0.02 |
| 51 | | 0.755 | 1.35 | 2.33 | 0.369 | 0.000990 | 5.05 | 3.00 | 0.000 | -3.81 | 0.012 |
| 52 | | 0.746 | 1.67 | 2.41 | 0.360 | 0.000990 | 5.12 | 2.67 | 0.167 | -3.81 | 0.012 |
| 53 | | 0.734 | 2.15 | 2.53 | 0.348 | 0.000990 | 5.22 | 2.33 | 0.333 | -3.81 | 0.012 |
| 54 | | 0.717 | 3.02 | 2.72 | 0.331 | 0.000990 | 5.35 | 2.00 | 0.500 | -3.81 | 0.012 |
| 55 | | 0.691 | 4.86 | 3.03 | 0.308 | 0.000990 | 5.54 | 1.67 | 0.667 | -3.81 | 0.012 |
| 56 | | 0.646 | 10.72 | 3.70 | 0.278 | 0.000990 | 5.77 | 1.34 | 0.833 | -3.81 | 0.012 |
| 57 | B\ Cv11.31 | 0.692 | 1.80 | 3.02 | 0.278 | 0.000990 | 5.78 | 3.00 | 0.000 | -11.31 | 0.01 |
| 58 | | 0.677 | 2.53 | 3.22 | 0.263 | 0.000990 | 5.89 | 2.50 | 0.083 | -11.31 | 0.01 |
| 59 | | 0.657 | 4.07 | 3.52 | 0.246 | 0.000990 | 6.03 | 2.00 | 0.167 | -11.31 | 0.01 |
| 60 | | 0.610 | 9.71 | 4.40 | 0.205 | 0.000990 | 6.36 | 1.50 | 0.250 | -11.31 | 0.01 |
| 61 | | 0.743 | 1.42 | 2.43 | 0.351 | 0.000990 | 5.19 | 3.00 | 0.000 | -11.31 | 0.01 |
| 62 | | 0.734 | 1.93 | 2.53 | 0.345 | 0.000990 | 5.24 | 2.50 | 0.083 | -11.31 | 0.01 |
| 63 | | 0.721 | 2.96 | 2.67 | 0.338 | 0.000990 | 5.30 | 2.00 | 0.167 | -11.31 | 0.01 |
| 64 | | 0.683 | 6.39 | 3.14 | 0.312 | 0.000990 | 5.50 | 1.50 | 0.250 | -11.31 | 0.01 |
| 65 | | 0.745 | 1.41 | 2.42 | 0.354 | 0.000990 | 5.17 | 3.00 | 0.000 | -11.31 | 0.012 |
| 66 | | 0.734 | 1.93 | 2.53 | 0.345 | 0.000990 | 5.24 | 2.50 | 0.083 | -11.31 | 0.012 |
| 67 | | 0.715 | 3.04 | 2.73 | 0.329 | 0.000990 | 5.37 | 2.00 | 0.167 | -11.31 | 0.012 |
| 68 | | 0.669 | 6.92 | 3.33 | 0.288 | 0.000990 | 5.69 | 1.50 | 0.250 | -11.31 | 0.012 |
| 69 | | 0.832 | 0.95 | 1.74 | 0.524 | 0.000990 | 3.81 | 3.00 | 0.000 | -11.31 | 0.012 |
| 70 | | 0.820 | 1.28 | 1.81 | 0.522 | 0.000990 | 3.82 | 2.50 | 0.083 | -11.31 | 0.012 |
| 71 | | 0.799 | 1.93 | 1.96 | 0.519 | 0.000990 | 3.85 | 2.00 | 0.167 | -11.31 | 0.012 |
| 72 | | 0.749 | 3.90 | 2.38 | 0.511 | 0.000990 | 3.91 | 1.50 | 0.250 | -11.31 | 0.012 |
| 73 | | 0.835 | 0.94 | 1.72 | 0.531 | 0.000990 | 3.75 | 3.00 | 0.000 | -11.31 | 0.016 |
| 74 | | 0.821 | 1.27 | 1.81 | 0.525 | 0.000990 | 3.80 | 2.50 | 0.083 | -11.31 | 0.016 |
| 75 | | 0.800 | 1.92 | 1.95 | 0.521 | 0.000990 | 3.83 | 2.00 | 0.167 | -11.31 | 0.016 |
| 76 | | 0.747 | 3.98 | 2.40 | 0.501 | 0.000990 | 3.99 | 1.50 | 0.250 | -11.31 | 0.016 |
| 77 | | 0.834 | 0.94 | 1.72 | 0.530 | 0.000990 | 3.76 | 3.00 | 0.000 | -11.31 | 0.016 |
| 78 | | 0.821 | 1.27 | 1.81 | 0.525 | 0.000990 | 3.80 | 2.50 | 0.083 | -11.31 | 0.016 |
| 79 | | 0.798 | 1.95 | 1.97 | 0.513 | 0.000990 | 3.90 | 2.00 | 0.167 | -11.31 | 0.016 |
| 80 | | 0.745 | 4.08 | 2.42 | 0.489 | 0.000990 | 4.09 | 1.50 | 0.250 | -11.31 | 0.016 |
| 81 | B | 0.624 | 12.46 | 4.11 | 0.241 | 0.000990 | 6.07 | 1.33 | 0.167 | 3.81 | 0.012 |

| | | | | | | | | | | |
|---|---|---|---|---|---|---|---|---|---|---|
| 82 | et al\ D | 0.648 | 6.15 | 3.68 | 0.244 | 0.000990 | 6.05 | 1.67 | 0.333 | 3.81 | 0.012 |
| 83 | | 0.652 | 4.18 | 3.60 | 0.240 | 0.000990 | 6.08 | 2.00 | 0.500 | 3.81 | 0.012 |
| 84 | | 0.649 | 3.25 | 3.66 | 0.231 | 0.000990 | 6.15 | 2.33 | 0.667 | 3.81 | 0.012 |
| 85 | | 0.636 | 2.80 | 3.89 | 0.214 | 0.000990 | 6.29 | 2.66 | 0.833 | 3.81 | 0.012 |
| 86 | | 0.644 | 2.26 | 3.74 | 0.222 | 0.000990 | 6.23 | 3.00 | 1.000 | 3.81 | 0.012 |
| 87 | | 0.662 | 9.69 | 3.45 | 0.310 | 0.000990 | 5.52 | 1.33 | 0.167 | 3.81 | 0.012 |
| 88 | | 0.699 | 4.67 | 2.93 | 0.322 | 0.000990 | 5.43 | 1.67 | 0.333 | 3.81 | 0.012 |
| 89 | | 0.714 | 3.06 | 2.74 | 0.327 | 0.000990 | 5.38 | 2.00 | 0.500 | 3.81 | 0.012 |
| 90 | | 0.722 | 2.28 | 2.65 | 0.329 | 0.000990 | 5.36 | 2.33 | 0.667 | 3.81 | 0.012 |
| 91 | | 0.722 | 1.86 | 2.66 | 0.323 | 0.000990 | 5.42 | 2.66 | 0.833 | 3.81 | 0.012 |
| 92 | | 0.730 | 1.51 | 2.57 | 0.331 | 0.000990 | 5.35 | 3.00 | 1.000 | 3.81 | 0.012 |
| 93 | | 0.644 | 10.97 | 3.75 | 0.274 | 0.000990 | 5.81 | 1.33 | 0.167 | 3.81 | 0.016 |
| 94 | | 0.704 | 4.54 | 2.87 | 0.331 | 0.000990 | 5.36 | 1.67 | 0.333 | 3.81 | 0.016 |
| 95 | | 0.721 | 2.95 | 2.66 | 0.339 | 0.000990 | 5.29 | 2.00 | 0.500 | 3.81 | 0.016 |
| 96 | | 0.730 | 2.20 | 2.57 | 0.341 | 0.000990 | 5.27 | 2.33 | 0.667 | 3.81 | 0.016 |
| 97 | | 0.732 | 1.78 | 2.55 | 0.338 | 0.000990 | 5.30 | 2.66 | 0.833 | 3.81 | 0.016 |
| 98 | | 0.740 | 1.45 | 2.47 | 0.346 | 0.000990 | 5.24 | 3.00 | 1.000 | 3.81 | 0.016 |
| 99 | | 0.620 | 12.80 | 4.20 | 0.235 | 0.000990 | 6.12 | 1.33 | 0.167 | 3.81 | 0.02 |
| 100 | | 0.683 | 5.10 | 3.14 | 0.295 | 0.000990 | 5.64 | 1.67 | 0.333 | 3.81 | 0.02 |
| 101 | | 0.710 | 3.13 | 2.80 | 0.320 | 0.000990 | 5.44 | 2.00 | 0.500 | 3.81 | 0.02 |
| 102 | | 0.725 | 2.25 | 2.62 | 0.334 | 0.000990 | 5.33 | 2.33 | 0.667 | 3.81 | 0.02 |
| 103 | | 0.742 | 1.70 | 2.45 | 0.354 | 0.000990 | 5.17 | 2.66 | 0.833 | 3.81 | 0.02 |
| 104 | | 0.738 | 1.46 | 2.49 | 0.342 | 0.000990 | 5.26 | 3.00 | 1.000 | 3.81 | 0.02 |
| 105 | | 0.709 | 6.09 | 2.81 | 0.493 | 0.000990 | 4.06 | 1.33 | 0.167 | 3.81 | 0.016 |
| 106 | | 0.770 | 2.97 | 2.19 | 0.506 | 0.000990 | 3.95 | 1.67 | 0.333 | 3.81 | 0.016 |
| 107 | | 0.798 | 1.95 | 1.97 | 0.514 | 0.000990 | 3.89 | 2.00 | 0.500 | 3.81 | 0.016 |
| 108 | | 0.812 | 1.46 | 1.87 | 0.513 | 0.000990 | 3.89 | 2.33 | 0.667 | 3.81 | 0.016 |
| 109 | | 0.824 | 1.16 | 1.79 | 0.519 | 0.000990 | 3.85 | 2.66 | 0.833 | 3.81 | 0.016 |
| 110 | | 0.832 | 0.95 | 1.73 | 0.525 | 0.000990 | 3.80 | 3.00 | 1.000 | 3.81 | 0.016 |
| 111 | | 0.709 | 6.01 | 2.80 | 0.499 | 0.000990 | 4.00 | 1.33 | 0.167 | 3.81 | 0.02 |
| 112 | | 0.769 | 2.99 | 2.20 | 0.503 | 0.000990 | 3.98 | 1.67 | 0.333 | 3.81 | 0.02 |
| 113 | | 0.797 | 1.96 | 1.97 | 0.512 | 0.000990 | 3.90 | 2.00 | 0.500 | 3.81 | 0.02 |
| 114 | | 0.812 | 1.47 | 1.87 | 0.512 | 0.000990 | 3.91 | 2.33 | 0.667 | 3.81 | 0.02 |
| 115 | | 0.822 | 1.16 | 1.80 | 0.516 | 0.000990 | 3.87 | 2.66 | 0.833 | 3.81 | 0.02 |
| 116 | | 0.828 | 0.97 | 1.76 | 0.515 | 0.000990 | 3.88 | 3.00 | 1.000 | 3.81 | 0.02 |
| 117 | B et al./ Dv5.71 | 0.638 | 11.38 | 3.85 | 0.264 | 0.000990 | 5.89 | 1.33 | 0.250 | 5.71 | 0.012 |
| 118 | | 0.670 | 5.47 | 3.33 | 0.275 | 0.000990 | 5.80 | 1.67 | 0.500 | 5.71 | 0.012 |
| 119 | | 0.682 | 3.60 | 3.16 | 0.278 | 0.000990 | 5.78 | 2.00 | 0.750 | 5.71 | 0.012 |
| 120 | | 0.681 | 2.78 | 3.17 | 0.270 | 0.000990 | 5.84 | 2.33 | 1.000 | 5.71 | 0.012 |
| 121 | | 0.670 | 9.12 | 3.33 | 0.329 | 0.000990 | 5.37 | 1.33 | 0.250 | 5.71 | 0.012 |
| 122 | | 0.709 | 4.40 | 2.80 | 0.341 | 0.000990 | 5.27 | 1.67 | 0.500 | 5.71 | 0.012 |
| 123 | | 0.726 | 2.89 | 2.61 | 0.347 | 0.000990 | 5.22 | 2.00 | 0.750 | 5.71 | 0.012 |

| | | | | | | | | | | | |
|---|---|---|---|---|---|---|---|---|---|---|---|
| 124 | | 0.731 | 2.18 | 2.56 | 0.344 | 0.000990 | 5.25 | 2.33 | 1.000 | 5.71 | 0.012 |
| 125 | | 0.675 | 8.79 | 3.25 | 0.342 | 0.000990 | 5.27 | 1.33 | 0.250 | 5.71 | 0.016 |
| 126 | | 0.716 | 4.25 | 2.73 | 0.353 | 0.000990 | 5.17 | 1.67 | 0.500 | 5.71 | 0.016 |
| 127 | | 0.740 | 2.69 | 2.47 | 0.373 | 0.000990 | 5.02 | 2.00 | 0.750 | 5.71 | 0.016 |
| 128 | | 0.743 | 2.06 | 2.43 | 0.364 | 0.000990 | 5.09 | 2.33 | 1.000 | 5.71 | 0.016 |
| 129 | | 0.660 | 9.80 | 3.48 | 0.307 | 0.000990 | 5.55 | 1.33 | 0.250 | 5.71 | 0.02 |
| 130 | | 0.711 | 4.36 | 2.78 | 0.344 | 0.000990 | 5.25 | 1.67 | 0.500 | 5.71 | 0.02 |
| 131 | | 0.740 | 2.69 | 2.47 | 0.373 | 0.000990 | 5.02 | 2.00 | 0.750 | 5.71 | 0.02 |
| 132 | | 0.754 | 1.96 | 2.33 | 0.383 | 0.000990 | 4.93 | 2.33 | 1.000 | 5.71 | 0.02 |
| 133 | | 0.710 | 5.79 | 2.79 | 0.519 | 0.000990 | 3.85 | 1.33 | 0.250 | 5.71 | 0.016 |
| 134 | | 0.775 | 2.84 | 2.15 | 0.529 | 0.000990 | 3.77 | 1.67 | 0.500 | 5.71 | 0.016 |
| 135 | | 0.804 | 1.86 | 1.92 | 0.538 | 0.000990 | 3.70 | 2.00 | 0.750 | 5.71 | 0.016 |
| 136 | | 0.821 | 1.39 | 1.81 | 0.539 | 0.000990 | 3.69 | 2.33 | 1.000 | 5.71 | 0.016 |
| 137 | | 0.710 | 5.76 | 2.79 | 0.522 | 0.000990 | 3.83 | 1.33 | 0.250 | 5.71 | 0.02 |
| 138 | | 0.776 | 2.79 | 2.14 | 0.537 | 0.000990 | 3.70 | 1.67 | 0.500 | 5.71 | 0.02 |
| 139 | | 0.804 | 1.86 | 1.92 | 0.537 | 0.000990 | 3.70 | 2.00 | 0.750 | 5.71 | 0.02 |
| 140 | | 0.820 | 1.40 | 1.81 | 0.537 | 0.000990 | 3.70 | 2.33 | 1.000 | 5.71 | 0.02 |
| 141./ | Y et al /Dv3.81 | 0.305 | 20.60 | 35.09 | 0.146 | 0.000880 | 1.90 | 1.33 | 0.167 | 3.81 | 0.041 |
| 142 | | 0.384 | 10.37 | 17.69 | 0.145 | 0.000880 | 1.90 | 1.67 | 0.333 | 3.81 | 0.041 |
| 143 | | 0.446 | 6.65 | 11.24 | 0.151 | 0.000880 | 1.89 | 2.00 | 0.500 | 3.81 | 0.041 |
| 144 | | 0.500 | 4.76 | 7.98 | 0.158 | 0.000880 | 1.87 | 2.33 | 0.667 | 3.81 | 0.041 |
| 145 | | 0.552 | 3.59 | 5.94 | 0.167 | 0.000880 | 1.85 | 2.66 | 0.833 | 3.81 | 0.041 |
| 146 | | 0.594 | 2.91 | 4.78 | 0.172 | 0.000880 | 1.84 | 3.00 | 1.000 | 3.81 | 0.041 |
| 147 | | 0.432 | 8.83 | 12.44 | 0.340 | 0.000880 | 1.47 | 1.33 | 0.167 | 3.81 | 0.0615 |
| 148 | | 0.548 | 4.34 | 6.09 | 0.346 | 0.000880 | 1.45 | 1.67 | 0.333 | 3.81 | 0.0615 |
| 149 | | 0.631 | 2.85 | 3.99 | 0.351 | 0.000880 | 1.44 | 2.00 | 0.500 | 3.81 | 0.0615 |
| 150 | | 0.696 | 2.13 | 2.97 | 0.353 | 0.000880 | 1.44 | 2.33 | 0.667 | 3.81 | 0.0615 |
| 151 | | 0.754 | 1.67 | 2.33 | 0.359 | 0.000880 | 1.42 | 2.66 | 0.833 | 3.81 | 0.0615 |
| 152 | | 0.806 | 1.37 | 1.91 | 0.364 | 0.000880 | 1.41 | 3.00 | 1.000 | 3.81 | 0.0615 |
| 153 | Y et al/ Dv 11.31 | 0.372 | 11.41 | 19.43 | 0.146 | 0.000880 | 1.90 | 1.60 | 0.100 | 11.31 | 0.041 |
| 154 | | 0.450 | 6.51 | 10.97 | 0.154 | 0.000880 | 1.88 | 2.00 | 0.167 | 11.31 | 0.041 |
| 155 | | 0.534 | 3.92 | 6.56 | 0.159 | 0.000880 | 1.87 | 2.60 | 0.267 | 11.31 | 0.041 |
| 156 | | 0.576 | 3.14 | 5.25 | 0.159 | 0.000880 | 1.87 | 3.00 | 0.333 | 11.31 | 0.041 |
| 157 | | 0.526 | 4.89 | 6.87 | 0.341 | 0.000880 | 1.46 | 1.60 | 0.100 | 11.31 | 0.0615 |
| 158 | | 0.630 | 2.85 | 4.00 | 0.351 | 0.000880 | 1.44 | 2.00 | 0.167 | 11.31 | 0.0615 |
| 159 | | 0.741 | 1.76 | 2.46 | 0.355 | 0.000880 | 1.43 | 2.60 | 0.267 | 11.31 | 0.0615 |
| 160 | | 0.801 | 1.39 | 1.94 | 0.359 | 0.000880 | 1.42 | 3.00 | 0.333 | 11.31 | 0.0615 |
| 161 | NK/ Cv 5 | 0.584 | 8.02 | 5.01 | 0.156 | 0.001100 | 4.22 | 1.80 | 0.000 | -5 | 0.037 |
| 162 | | 0.547 | 10.37 | 6.09 | 0.126 | 0.001100 | 4.37 | 1.77 | 0.044 | -5 | 0.037 |
| 163 | | 0.527 | 21.08 | 6.85 | 0.118 | 0.001100 | 4.41 | 1.40 | 0.500 | -5 | 0.037 |
| 164 | | 0.678 | 4.76 | 3.21 | 0.262 | 0.001100 | 3.69 | 1.80 | 0.000 | -5 | 0.04 |
| 165 | | 0.640 | 6.10 | 3.81 | 0.214 | 0.001100 | 3.93 | 1.77 | 0.044 | -5 | 0.04 |

| | | | | | | | | | | | |
|---|---|---|---|---|---|---|---|---|---|---|---|
| 166 | | 0.617 | 11.72 | 4.26 | 0.213 | 0.001100 | 3.94 | 1.40 | 0.500 | -5 | 0.04 |
| 167 | | 0.701 | 4.18 | 2.90 | 0.299 | 0.001100 | 3.51 | 1.80 | 0.000 | -5 | 0.043 |
| 168 | | 0.682 | 4.83 | 3.15 | 0.271 | 0.001100 | 3.65 | 1.77 | 0.044 | -5 | 0.043 |
| 169 | | 0.646 | 9.60 | 3.71 | 0.260 | 0.001100 | 3.70 | 1.40 | 0.500 | -5 | 0.043 |
| 170 | | 0.716 | 3.85 | 2.73 | 0.325 | 0.001100 | 3.37 | 1.80 | 0.000 | -5 | 0.045 |
| 171 | | 0.697 | 4.43 | 2.95 | 0.295 | 0.001100 | 3.52 | 1.77 | 0.044 | -5 | 0.045 |
| 172 | | 0.660 | 8.67 | 3.48 | 0.288 | 0.001100 | 3.56 | 1.40 | 0.500 | -5 | 0.045 |
| 173 | NK/ Cv 9 | 0.593 | 7.65 | 4.80 | 0.163 | 0.001100 | 4.18 | 1.80 | 0.000 | -9 | 0.032 |
| 174 | | 0.588 | 8.48 | 4.92 | 0.160 | 0.001100 | 4.20 | 1.74 | 0.079 | -9 | 0.032 |
| 175 | | 0.573 | 15.59 | 5.31 | 0.160 | 0.001100 | 4.20 | 1.40 | 0.500 | -9 | 0.032 |
| 176 | | 0.659 | 5.30 | 3.50 | 0.236 | 0.001100 | 3.82 | 1.80 | 0.000 | -9 | 0.035 |
| 177 | | 0.655 | 5.79 | 3.55 | 0.234 | 0.001100 | 3.83 | 1.74 | 0.079 | -9 | 0.035 |
| 178 | | 0.614 | 11.95 | 4.32 | 0.209 | 0.001100 | 3.96 | 1.40 | 0.500 | -9 | 0.035 |
| 179 | | 0.683 | 4.65 | 3.15 | 0.269 | 0.001100 | 3.66 | 1.80 | 0.000 | -9 | 0.038 |
| 180 | | 0.677 | 5.12 | 3.22 | 0.265 | 0.001100 | 3.67 | 1.74 | 0.079 | -9 | 0.038 |
| 181 | | 0.639 | 10.11 | 3.84 | 0.247 | 0.001100 | 3.77 | 1.40 | 0.500 | -9 | 0.038 |
| 182 | | 0.712 | 3.94 | 2.77 | 0.317 | 0.001100 | 3.41 | 1.80 | 0.000 | -9 | 0.041 |
| 183 | | 0.709 | 4.25 | 2.81 | 0.319 | 0.001100 | 3.40 | 1.74 | 0.079 | -9 | 0.041 |
| 184 | | 0.667 | 8.18 | 3.37 | 0.305 | 0.001100 | 3.48 | 1.40 | 0.500 | -9 | 0.041 |
| 185 | NK/ Cv 13.38 | 0.601 | 7.32 | 4.62 | 0.171 | 0.001100 | 4.15 | 1.80 | 0.000 | -13.38 | 0.031 |
| 186 | | 0.575 | 9.52 | 5.27 | 0.149 | 0.001100 | 4.25 | 1.70 | 0.119 | -13.38 | 0.031 |
| 187 | | 0.516 | 22.59 | 7.26 | 0.111 | 0.001100 | 4.45 | 1.40 | 0.595 | -13.38 | 0.031 |
| 188 | | 0.630 | 6.23 | 4.01 | 0.201 | 0.001100 | 4.00 | 1.80 | 0.000 | -13.38 | 0.034 |
| 189 | | 0.622 | 7.26 | 4.16 | 0.195 | 0.001100 | 4.02 | 1.70 | 0.119 | -13.38 | 0.034 |
| 190 | | 0.591 | 13.87 | 4.84 | 0.180 | 0.001100 | 4.10 | 1.40 | 0.595 | -13.38 | 0.034 |
| 191 | | 0.679 | 4.73 | 3.19 | 0.264 | 0.001100 | 3.68 | 1.80 | 0.000 | -13.38 | 0.037 |
| 192 | | 0.665 | 5.68 | 3.40 | 0.250 | 0.001100 | 3.75 | 1.70 | 0.119 | -13.38 | 0.037 |
| 193 | | 0.638 | 10.12 | 3.84 | 0.247 | 0.001100 | 3.77 | 1.40 | 0.595 | -13.38 | 0.037 |
| 194 | | 0.715 | 3.86 | 2.73 | 0.324 | 0.001100 | 3.38 | 1.80 | 0.000 | -13.38 | 0.04 |
| 195 | | 0.707 | 4.45 | 2.83 | 0.319 | 0.001100 | 3.40 | 1.70 | 0.119 | -13.38 | 0.04 |
| 196 | | 0.669 | 8.04 | 3.34 | 0.311 | 0.001100 | 3.45 | 1.40 | 0.595 | -13.38 | 0.04 |